

Global Green Deal: International Cooperation on Net-Zero Carbon Emission

Chenghao Ding ^{*}, Clifford Singer [†] and Bei Yang [‡]

November 17, 2020

[Link to the latest version](#)

Abstract

We develop and estimate an integrated model of climate and the world economy to study international cooperation on net-zero carbon emission among sixteen geographic regions. We find that achieving net-zero emission by mid-century reduces global social welfare loss by up to 35%, accounting for the emission reduction cost. However, we show that the economic benefit of free-riding may entice each region to quit the cooperation at the early stage. We demonstrate that trigger strategies are not effective in stabilizing the cooperation and would quickly lead the world to the punishment phase. We also demonstrate that monetary transfers can improve the cooperation outcome but are not able to support net-zero emission. These results suggest that global effort on achieving net-zero carbon emission by mid-century is desirable, but the required international cooperation may be difficult to sustain.

1 Introduction

Despite the international consensus that it is necessary to mitigate climate change, we have not seen significant progress since the Paris Agreement in 2012. We are still on a fast track of global warming. In most scientific projections, increase in global average temperature over the pre-industrial level will be at least 3 °C before this century ends. To meet the Paris Agreement's

^{*}Department of Nuclear, Plasma, and Radiological Engineering, University of Illinois, Urbana, IL USA 61801.
email: cd7@illinois.edu.

[†]Department of Nuclear, Plasma, and Radiological Engineering, University of Illinois, Urbana, IL USA 61801.
email: csinger@illinois.edu.

[‡]Department of Economics, University of Illinois, Urbana, IL USA 61801. *email:* beiyang2@illinois.edu (*corresponding author*).

goal of limiting temperature increase well below 2 °C, we must have a deep cut in global greenhouse gas emission in the upcoming decades. In the United Nation’s 2019 Climate Action Summit, the European Union (EU) made an encouraging announcement: it plans to become the first climate-neutral continent with a series of action plans called the European Green Deal¹. The highlight of this proposal is to cut greenhouse gas emission to net-zero by 2050. China recently² has also announced in the United Nation’s general assembly that it pledges to accomplish the same goal by 2060. Despite the ambitious goal of the EU and China, climate change is still a global problem that needs a global solution.

In this paper, we investigate the economic incentives for cooperation among sixteen geographic regions on achieving net-zero carbon dioxide (CO₂) emission by mid-century. In particular, we address three questions in order. First, is net-zero emission by mid-century worth pursuing as a global target based on economic incentives? Second, if such cooperation is worth pursuing but may be compromised by the free-riding incentives, are trigger strategies effective in sustaining cooperation as suggested in the literature? Third, can transfer payments improve the cooperation outcome? Using these questions to guide our inquiry, we aim to provide insights on the potential obstacles to achieving a global green-economy by mid-century.

To answer these questions, we develop and estimate an integrated model of climate and the economy based on independent studies on global climate dynamics, climate change impacts and emission reduction costs. This approach allows us to use the social welfare of future consumptions as a well-defined measure for economic incentives, so that we can reliably estimate the benefits and study the stability of the global cooperation. While this allows us to gain important insights for our research questions that cannot be obtained from a more stylized game-theoretic model, it becomes mathematically challenging to solve the model explicitly. To overcome this difficulty, we first develop an analytic approximation for the social welfare that can be computed numerically, and then we rely on game-theoretic insights to design policy simulations in order to properly address the research questions.

This paper continues the line of work of using integrated assessment models (IAMs)³ to address

¹https://ec.europa.eu/info/strategy/priorities-2019-2024/european-green-deal_en.

²<https://www.economist.com/china/2020/09/24/china-aims-to-cut-its-net-carbon-dioxide-emissions-to-zero-by-2060>.

³See Nordhaus 2013 for a survey

questions related to climate change. The most similar IAM to our model is the RICE model⁴ in [Nordhaus and Yang 1996](#) and [Nordhaus 2010](#). Although the main structure is similar, our model is different to the RICE model in terms of the specific model components and estimates. The climate module of our model is based on a series of studies originating in [Singer et al. 2008](#). While the current version of the RICE model uses quadratic functions with respect to global mean temperature to estimate climate change impacts, we developed a more detailed model based on [Anthoff and Tol 2014](#) that allows us to closely examine climate change impacts across regions. In addition, our model also allows for heterogenous emission reduction costs among regions.

The idea of using trigger strategies in sustaining climate cooperation has previously been studied in [Dockner et al. 1996](#), [Dutta and Radner 2009](#) and [Dutta and Radner 2010](#) using more stylized game-theoretical models. This paper complements their work by testing the effectiveness of trigger strategies using an integrated model that is backed by independent studies and up-to-date estimates. As we will show in this paper, trigger strategies may not be effective in deterring free-riding incentives due to the difference in climate change impacts across regions. This drawback of trigger strategies has not been emphasized in the previous work.

2 Integrated Model of Climate and the Economy

In this section, we first focus on highlighting the main structure of the model and then we will follow up with some discussion regarding certain model components, along with the studies and data we used in estimation. Finally we will describe the method for solving for the social welfare. To simplify notations, we will write a time-dependent variable $x(t)$ simply as x when we believe that the dependence on time is clear from the context. The term \dot{x} is exclusively used to represent the first-order derivative of $x(t)$ with respect to time. In addition, we will use $x(t)$ and x_t to remind us whether the variable is endogenous or exogenous in the context of discussion, respectively.

2.1 Description of the Model

The model runs in continuous time from the reference year $t_0 = 2020$ to infinity, and in which we divide the world into sixteen geographic regions.

⁴Regional Dynamic Integrated model of Climate and the Economy.

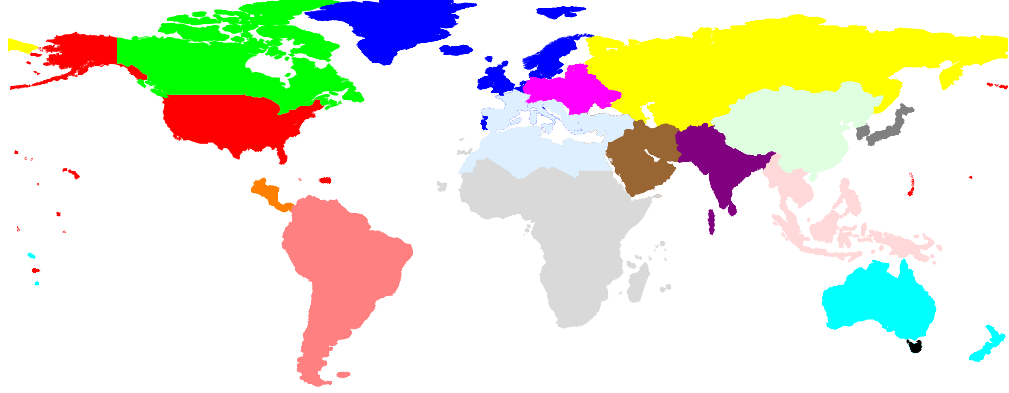


Figure 1: Sixteen geographic regions in the climate-economic model. The list of countries in each region is provided in Appendix A.

Through out the paper, we will make reference to a benchmark called the “No-New-Policy” scenario. It depicts a world in which carbon emissions and the associated climate change will follow the pre-2020 trend. We use \hat{E}_i to represent the “No-New-Policy” emission for each region i . The region’s emission reduction policy, denoted by a_i , is a sequence of reduction rates. After adopting the new policy, region i ’s actual emissions become:

$$E_i(t) = (1 - a_i(t)) \times \hat{E}_{i,t}. \quad (1)$$

We assume that each region has perfect control to implement the corresponding emission reduction through the use of region-wide carbon tax, cap-and-trade programs, Carbon Dioxide Removal (CDR) technologies, or policies that encourages production with cleaner technologies etc.,.

We model global climate dynamics by focusing on two variables that are directly affected by carbon emission: the atmospheric carbon content level c_a and the global mean temperature τ , each computed as increments over their respective pre-industrial levels⁵. Emitted CO₂ that enters the atmosphere increases the carbon content level, while the existing carbon content diminishes naturally albeit at a slow pace. This simple carbon dynamic is captured by the following carbon balance equation:

⁵We also keep track of the sea-level rise and ocean acidification. Dynamics of these two variables are described in Appendix C.5 and C.6, respectively.

$$\dot{c}_a(t) = \underbrace{\left(\alpha_1 + (1 - \alpha_1) \cdot \frac{c_a(t)}{c_a(t) + \alpha_2 \cdot \alpha_3} \right)}_{\text{Atmospheric retention fraction}} \times \sum_i E_i(t) - \underbrace{\frac{c_a(t)}{\alpha_4}}_{\text{Natural clearance of CO}_2}. \quad (2)$$

The atmospheric retention fraction in the equation is less than one because the upper-layer ocean absorbs a portion of emitted carbon. However, as carbon content accumulates in the atmosphere, CO₂ concentration in the upper ocean increases as well. This in turn lowers the ocean's ability to retain emitted carbon and thus increase atmospheric retention fraction in the future.

The dynamic of global mean temperature is modeled by a linear heat balance equation in which consistent change in temperature is driven by changes in the net incoming radiative forcing of the Earth. Carbon emissions produce CO₂ that, as a type of greenhouse gas, has the property of reradiating outgoing heat energy back to the Earth surface which in turn increases the net incoming radiative forcing:

$$\alpha_5 \dot{\tau}(t) = \underbrace{\alpha_6 \ln \left(1 + \frac{c_a(t)}{\alpha_2} \right)}_{\text{CO}_2\text{-driven radiative forcing}} + F_t - \frac{\tau(t)}{\alpha_7}. \quad (3)$$

The exogenous variable F in the heat balance equation is the total radiative forcing that accounts for those driven by other greenhouse gases, long-term variation in solar irradiance, changes in radiative shielding of albedo due to land use changes etc.,.

To model the economic response, we modify the standard *Ramsey-Cass-Koopmans model*⁶ by introducing climate change impacts and emission reduction costs as perturbations to each region's total production function. Each region's background economy has a Cobb-Douglas production function with Hicks-neutral technological progress that takes labor and capital as inputs to produce a single commodity. We treat each region's total productivity A_i and labor input L_i as exogenous variables while the capital stock K_i is endogenously determined. The climate change impact, denoted by $\Omega(c_a(t), \tau(t), Z_{i,t}^\Omega)$, is determined by global climate while the emission reduction cost, denoted by $\Lambda(a_i(t), Z_{i,t}^\Lambda)$, is determined by each region's own reduction policy, and Z_i^Ω and Z_i^Λ are collections of region-specific exogenous variables. The climate change impact and emission reduction cost are treated as perturbations in the production function that in turn determines the actual output:

⁶Ramsey 1928; Cass 1965; Koopmans 1963.

$$\underbrace{Y_i(t)}_{\text{Actual output}} = \underbrace{(1 + \Omega_i(t) - \Lambda_i(t))}_{\text{Climate-related perturbation}} \times A_{i,t} L_{i,t}^\omega K_i(t)^{1-\omega}. \quad (4)$$

Given the perturbed production function, each region's economy optimally divide the actual output between consumption, denoted by C_i , and investment in capital stock in order to achieve maximal social welfare given the available resources. Each region's social welfare W_i is the total present value of all future instantaneous utilities that are proportional to the exogenously given population P_i and have diminishing marginal utility of per capita consumption. In particular, we assume:

$$W_i = \max_{C_i} \int_{t_0}^{\infty} P_{i,t} \underbrace{\frac{(C_i(t)/P_{i,t})^{1-\theta}}{1-\theta}}_{\text{Instantaneous utilities}} e^{-\rho(t-t_0)} dt, \quad (5)$$

$$\text{s.t.} \quad Y_i(t) = \underbrace{\dot{K}_i(t) + rK_i(t)}_{\text{Investment}} + \underbrace{C_i(t)}_{\text{Consumption}}.$$

The economic incentive for each region is then measured by the regional social welfare, and we define the global welfare as the sum of all sixteen regions' social welfare.

2.2 Estimation and Data

2.2.1 “No-New-Policy” Emissions and the Background Economy

We extrapolate the “No-New-Policy” carbon emissions in two steps (Appendix B.1). We first extrapolate, based on Ding (2018), the global carbon emission using an analytic function that in turn is divided into that from industrial activities and that from land-use changes. The industrial emission is fitted to a logistic function since it both captures the early exponential growth of emission and accounts for finiteness of fossil fuel resources that prevents the industrial emission from growing in a linear or faster way indefinitely. Historically, the deforestation has been a significant contribution to carbon emissions from land-use changes. Since the amount of forested land is finite, the total emission from deforestation must decline over time. Hence, we fit the cumulative emission from land-use changes by a logistic function. In the second step, we then extrapolate the fraction in global carbon emission for each region based on the country-level carbon emission data for 1965-2018 from the BP Statistical Review of World Energy⁷ and Marilena et al. (2018).

⁷<https://www.bp.com/en/global/corporate/energy-economics/statistical-review-of-world-energy.html>, accessed on January 10, 2020.

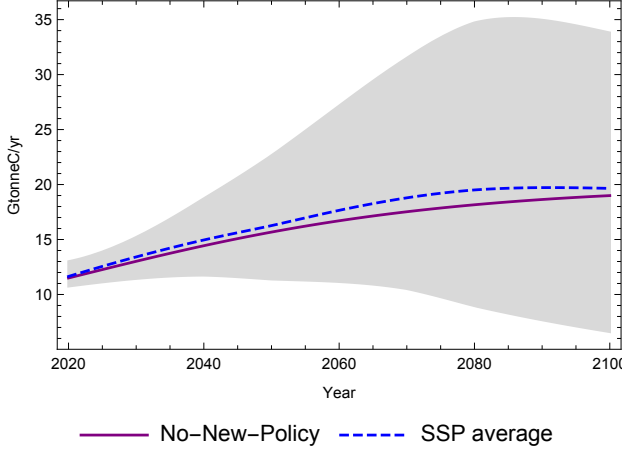


Figure 2: Extrapolated global carbon emission under the “No-New-Policy” scenario (purple line) compared to projection of IAM “marker” baseline scenarios (gray area, and blue dashed line represents the average) in SSP database from Riahi et al. (2017).

For the regional background economy (Appendix B.2), we assume that the total productivity A_r and the labor inputs L_r are proportional to logistic functions and are region-specific, and calibrate the parameter values against long-term historical data from Maddison⁸, International Monetary Fund⁹ and United Nations¹⁰. Table 1 below shows the values for the global constants of the background economy that are based on calibration provided in Singer et al. (2008).

Table 1: Global constants and calibrated values for the background economy

Symbol	Value	Units	Description
ω	0.675	-	Labor share of production
θ	1.345	-	Consumption elasticity of marginal welfare
ρ	2.300	%	Social discount rate
r	0.106	-	Capital depreciation rate

Note: Parameter values of the above global constants are the mean values of data-calibrated probability distributions provided in Singer et al. (2008).

2.2.2 Climate Balance Equations

The carbon balance equation and associated parameter values in Table 2 are based on Singer and Matchett (2015). This equation reproduces well the results from a more complex four-chamber

⁸<https://www.rug.nl/ggdc/historicaldevelopment/maddison/releases/maddison-project-database-2018>, accessed August 22, 2019.

⁹<https://www.imf.org/external/pubs/ft/weo/2019/02/weodata/index.aspx>, accessed February 15, 2020. See

¹⁰<https://population.un.org/wpp/>, accessed August 24, 2019.

carbon balance model used in Singer et al. (2008) and Singer et al. (2014). We simplify the equation by omitting the comparatively small feedback effect from temperature that would otherwise slightly affect the atmospheric retention fraction of emitted carbon. This simplification allows us to decouple the otherwise paired nonlinear differential equations for the global mean temperature and the atmospheric carbon content. It is worth mentioning that the long term natural decrease rate of the existing atmospheric carbon content is qualitatively known to be very small but the quantitative value is not precisely known. This parameter value in Table 2 can thus only be treated as expert's guess.

The heat balance equation and the associated parameter values in Table 2 are modified and calibrated based on Milligan (2012) and Ding (2018). Linearization of this equation allows us to avoid keeping track of all other radiative forces included in F and instead only calculate the changes in global mean temperature caused by the regions' emission reduction policies. Let $\hat{\tau}$ be the "No-New-Policy" global mean temperature and define the difference in temperatures as

$$\Delta\tau(t) := \underbrace{\tau(t)}_{\text{Actual temperature}} - \underbrace{\hat{\tau}(t)}_{\text{"No-New-Policy" temperature}}. \quad (6)$$

Linearity of equation (3) implies

$$\alpha_5 \Delta\hat{\tau}(t) = \underbrace{\alpha_6 \ln \left(\frac{c_a(t)}{\hat{c}_a(t)} \right)}_{\text{Change in CO}_2\text{-driven radiative forcing}} - \frac{\Delta\tau(t)}{\alpha_7}, \quad (7)$$

where \hat{c}_a is the "No-New-Policy" carbon content level in the atmosphere. Using the collection of emission reduction policies and the extrapolated "No-New-Policy" carbon emissions as inputs, we can first calculate the actual and "No-New-Policy" carbon content levels using the carbon balance equation. Combining it with the extrapolated "No-New-Policy" global mean temperature (see Appendix B.3), we can calculate the difference in global temperature $\Delta\tau$ by numerically integrating the above differential equation and thus obtain the actual global mean temperature τ .

Table 2: Parameters and the associated values for in carbon and heat balance equations

Symbol	Value	Units	Description
α_1	0.37	-	Pre-industrial atmospheric retention fraction of carbon emissions
α_2	0.59	TtonneC	Pre-industrial atmospheric carbon content
α_3	0.50	-	Ocean mixed layer CO ₂ saturation parameter
α_4	1320	years	Atmospheric carbon clearance timescale
α_5	24.1	(W/m ²) yr/°C	Thermal inertia constant
α_6	5.35	W/m ²	CO ₂ -driven radiative forcing parameter
α_7	0.63	°C/(W/m ²)	Climate sensitivity

2.2.3 Climate Change Impacts

Our priority in constructing an assessment of the climate change impact is that it must be sufficiently realistic but tractable enough so that it can be updated in future work in the presence of new findings and evidences (Appendix C). Among various models reviewed by [Stanton et al. \(2009\)](#) and [Gillingham et al. \(2018\)](#), many are too complex for our purpose. We thus choose [Anthoff and Tol \(2014\)](#) as the starting point. We divide the climate change impacts into eight categories: agriculture, forestry, water resources, heating-cooling-and-ventilation, dry-land protection associated with sea level rise, coral reef loss associated with ocean acidification, diseases and storm damages. Combining [Anthoff and Tol \(2014\)](#)'s model and various other studies, we first estimate the percentage impact within each category for each region and then maps those impacts to the percentage perturbation on each region's total production function. It is worth mentioning that in the assessment we take into account potential technological progresses that will gradually reduce some of these impacts over time. However, unless the current pace of climate change is slowed, Table 3 shows that all sixteen regions will still suffer from increasingly negative impact from climate change.

We emphasize that our climate change impact assessment is illustrative at best due to limited data, strong modeling assumptions and lack of empirical studies in some of the impact categories. As pointed out in the Intergovernmental Panel on Climate Change (IPCC)'s fifth assessment report, our “understanding of the regional nature of climate change, its impacts, regional and cross-regional vulnerabilities, and options for adaptation is still at a rudimentary level”¹¹. On the other hand, our assessment is consistent with the existing literature¹² in terms of quantitative magnitude that

¹¹https://www.ipcc.ch/site/assets/uploads/2018/02/WGIAR5-Chap21_FINAL.pdf, page-1184

¹²[Tol \(2018\)](#) provides a meta-analysis of existing climate change impact assessments.

Table 3: Climate change impact on regional productivity (%) under the “No-New-Policy” scenario

	2020	2040	2060	2080	2120		2020	2040	2060	2080	2120
Global mean temperature increase (°C)	1.0	1.6	2.3	2.7	3.8		1.0	1.6	2.3	2.7	3.8
Atmospheric CO ₂ concentration (ppm)	415	479	561	657	872		415	479	561	657	872
United States	0.08	0.02	-0.15	-0.26	-0.59	Central America	-0.02	-0.12	-0.42	-0.68	-1.58
Canada	0.16	0.10	-0.07	-0.21	-0.62	South America	-0.08	-0.23	-0.50	-0.71	-1.27
Western Europe	0.00	-0.10	-0.31	-0.48	-0.99	South Asia	-0.24	-0.32	-0.47	-0.61	-1.02
Japan and South Korea	0.10	0.13	0.12	0.08	-0.07	Southeast Asia	-0.26	-0.54	-0.91	-1.41	-1.88
Australia and New Zealand	0.15	0.12	0.07	0.02	-0.08	China Plus	0.40	-0.11	-0.53	-0.83	-1.83
Central and Eastern Europe	0.16	0.12	-0.08	-0.27	-0.87	North Africa	-1.96	-3.39	-5.10	-6.02	-8.77
Former Soviet Union	0.57	0.60	-0.01	-0.67	-2.88	Sub-Saharan Africa	-3.51	-4.47	-5.60	-6.34	-9.34
Middle East	-0.11	-0.27	-0.54	-0.74	-1.32	Small Island States	-0.17	-0.34	-0.64	-0.87	-1.53

Note: Temperate regions initially benefit from mild global warming. This is mainly due to reduced energy consumption for heating and increased productivity for agriculture.

climate change impacts are usually of a few percents of the total production when temperature increase is within 3 °C and in terms of the qualitative feature that poorer and tropical regions tend to be more vulnerable to climate change.

2.2.4 Emission Reduction Cost

Reduction in carbon emission from the “No-New-Policy” scenario can mainly be achieved by lowering the carbon intensity of output defined as

$$\hat{\sigma}_{i,t} := \frac{\hat{E}_{i,t}}{\hat{Y}_{i,t}}. \quad (8)$$

This goal can be accomplished by switching to non-carbon technology in energy production or lowering energy demand either from consumer side or from improvement of energy efficiency. However, as pointed out in [Gillingham and Stock \(2018\)](#), estimating emission reduction cost within each category tends to provide an inaccurate assessment. For example, the policy that encourages purchase of electric vehicles may decrease the gasoline fuel demand but increase the electricity demand, and the overall effect on emission depends on the carbon intensity in the region’s energy production. For this reason, we choose to not use the various engineering estimates of *marginal abatement cost curves*¹³. Instead, we opt for a more reduced-form approach in which we assume that the region’s reduction cost can be efficiently determined if it adopts a region-wide carbon tax or cap-and-trade

¹³US Energy Information Administration(2018): https://www.eia.gov/outlooks/aoe/pdf/electricity_generation.pdf; Lazard(2019): <https://www.lazard.com/perspective/lcoe2019>; McKinsey&Company(2013): <https://www.mckinsey.com/business-functions/sustainability/our-insights/pathways-to-a-low-carbon-economy>.

program.

The H.R. 2454, the American Clean Energy and Security Act of 2009 bill¹⁴ proposes a nationwide cap-and-trade program for the United States that intends to achieve 83% emission reduction in 2050 from the 2005 emission level¹⁵. Based on the U.S. Congressional Budget Office's estimates¹⁶, the percentage change in U.S. total production for adopting this cap-and-trade program can be approximated by the following analytic function:

$$\beta_1 \times a_i(t)^{\beta_2}, \quad (9)$$

where $\beta_1 = 3.12\%$ and $\beta_2 = 2.35$. This estimation is based on available technology of the United States in 2005. [Acemoglu et al. \(2016\)](#) shows that research subsidy and carbon tax can help encourage the production and innovation in cleaner technology, which will potentially change future reduction costs. [Nordhaus \(2010\)](#) implicitly assumes perfect spillover across regions of this effect so that all regions' reduction cost reduces at the same pace. However, as shown in [Harstad \(2012\)](#), the spillover of innovation in cleaner technology creates another ‘market-failure’, and without carefully designed international contracts all regions will invest at suboptimal level in the cleaner technology. We do not intend to solve this problem in this paper since it requires analyzing another layer of strategic interaction on top of the decisions regarding emission reductions. For this reason, we assume that innovations in cleaner technology will follow the pre-2020 trend so that the change in reduction cost for each region is proportional to its relative carbon intensity of output in the “No-New-Policy” scenario. More precisely, reduction cost function in our model takes the following form:

$$\Lambda_i(a_i(t), Z_{i,t}^{\Lambda}) = \beta_1 \left(\frac{\hat{\sigma}_{i,t}}{\hat{\sigma}_{\text{USA},2005}} \right) \times a_i(t)^{\beta_2}. \quad (10)$$

2.3 Method for Solving Social Welfare

Calculating the sixteen regions' social welfare requires us solving the optimization problem governing the consumption-investment decisions. Due to nonlinearity of the climate dynamics and complexity of the climate change impacts, it is difficult to obtain an exact solution. We thus develop

¹⁴<https://www.congress.gov/bill/111th-congress/house-bill/2454>.

¹⁵This is equivalent to an emission reduction rate of 87% for the USA region in our model.

¹⁶<https://www.cbo.gov/sites/default/files/111th-congress-2009-2010/reports/11-23-greenhousegasemissions-brief.pdf>.

an approximation for the solution that can be solved numerically. Our method uses an analytic approximation for the background economy derived in [Singer et al. \(2008\)](#) as the starting point.

Lemma 1 *Suppose the consumption C_i^0 is the solution of the optimization problem (5) when there is no climate change impacts nor emission reduction costs, i.e., $\Omega_i = \Lambda_i \equiv 0$, and the total productivity is proportional to a logistic function of the following form:*

$$A_{i,t} \propto \frac{1}{1 + e^{-(t-b_{2,i})/b_{3,i}}},$$

then the associated capital stock can be approximated by:

$$K_{i,t}^0 \approx \left(\frac{A_{i,t}}{1 + (1 - A_{i,t}) \cdot \frac{\theta}{\omega(\rho+r)b_{3,i}}} \right)^{\frac{1}{\omega}} \cdot L_{i,t},$$

and hence the consumption can be calculated by:

$$C_{i,t}^0 = A_{i,t}(K_{i,t}^0)^{1-\omega}L_{i,t}^\omega - rK_{i,t}^0 - \dot{K}_{i,t}^0.$$

We next combine the climate change impacts and emission reduction costs into a single variable D_i defined as:

$$\epsilon D_{i,t} := \Omega_{i,t} - \Lambda_{i,t}, \quad (11)$$

where we represent the sum of climate change impacts and abatement costs in percentage unit, i.e., $\epsilon = 0.01$. According to our assessment, climate change impacts and emission reduction costs are both relatively small perturbations on the sixteen regions' production functions. Therefore, this treatment helps us keep track of the magnitude of error terms in the approximation. Similarly, we can write the optimal consumption as

$$C_r^*(t) = (1 + \epsilon \gamma_r(t)) \times C_{r,t}^0, \quad (12)$$

and the associated capital stock as

$$K_r^*(t) = (1 + \epsilon \kappa_r(t)) \times K_{r,t}^0, \quad (13)$$

where γ_r and κ_r represent relative perturbations on consumption and capital stock, respectively.

Theorem 1 below characterizes an approximation for the optimal solution.

Theorem 1 *The relative perturbation terms γ_i and κ_i can be approximated, within the order of ϵ , by solving:*

$$\begin{cases} \theta\dot{\gamma}_i(t) = \left(\frac{(1-\omega)Y_{i,t}^0}{K_{i,t}^0}\right)D_{i,t} - \left(\frac{\omega(1-\omega)Y_{i,t}^0}{K_{i,t}^0}\right)\kappa_i(t); \\ \dot{\kappa}_i(t) = \left(\frac{Y_{i,t}^0}{K_{i,t}^0}\right)D_{i,t} + \left(\frac{-\omega Y_{i,t}^0 + C_{i,t}^0}{K_{i,t}^0}\right)\kappa_i(t) - \left(\frac{C_{i,t}^0}{K_{i,t}^0}\right)\gamma_i(t), \end{cases} \quad (14)$$

for the initial condition $\epsilon\kappa_i(t_0) = \frac{K_{i,t_0} - K_{i,t_0}^0}{K_{i,t_0}^0}$. In addition, supposing $\lim_{t \rightarrow \infty} D_{i,t} = \bar{D}_i$, we will also have the terminal condition:

$$\lim_{t \rightarrow \infty} \dot{\kappa}_i(t) = 0. \quad (15)$$

Proof. See Appendix D ■

The terminal condition (15) requires that the climate change impacts and emission abatement costs eventually being stabilized. Nordhaus and Yang (1996) and Nordhaus and Sztorc (2013) assume that there exists a backstop technology with decreasing cost such that productions of the world will no longer rely on the carbon technology around 2220. Although we do not assume such backstop technology in our model, we acknowledge that the world will eventually run out of fossil fuels and the carbon emissions will eventually decline. In addition, as shown in Rogner (1997), depletion of fluid fossil fuels increases the extraction cost that in turn will likely accelerate the decline in global carbon emissions even without the emission reduction policies. For this reason and for practical purpose, we assume that the long-term climate change impact will be fixed as constant after some finite (but large) time T if global carbon emissions have not achieved net-zero before then¹⁷. This empirical terminal condition, together with the pair of linear differential equations (14), allows us using the *implicit Runge-Kutta* method described in Press et al. (1992) to solve the problem numerically.

¹⁷The specific value of T depends on the context of analysis and is selected so that it has comparatively small effect on the conclusion.

3 Global Green Deal: Net-Zero Emission by Mid-Century

In this section, we address the first research question: is net-zero emission by mid-century, or a Global Green Deal, worth pursuing as a global target based on economic incentives? We begin by discussing how global emission reduction should be distributed over time and across regions, given the goal of achieving net-zero emission by mid-century. Then we describe the projected global climate, followed by examination and discussion on the economic incentives from both the global and individual region's perspectives.

3.1 Global Green Deal and Distribution of Burden

To begin with, we choose to use the European Green Deal as the leading example for the Global Green Deal. Besides the highlighted target of net-zero emission in 2050, the European Green Deal also intend to achieve 40% of emission reduction from its 2020 level within the next decade. This implies that the emission reduction rate for EU will increase at a faster pace in the early stage and slow down when it approaches one. This general feature is confirmed in our model, and verified through simulations not presented here, as the economically better choice for achieving net-zero emission by mid-century. The reason is that CO₂ emission reduction has a highly convex cost but a long-lasting impact on the global climate. A faster pace of reducing its emission at the early stage can thus achieve larger climate change mitigation at relatively low cost. Therefore, it is reasonable to use the European Green Deal as the global CO₂ emission reduction target for the Global Green Deal, as shown in Figure 3.

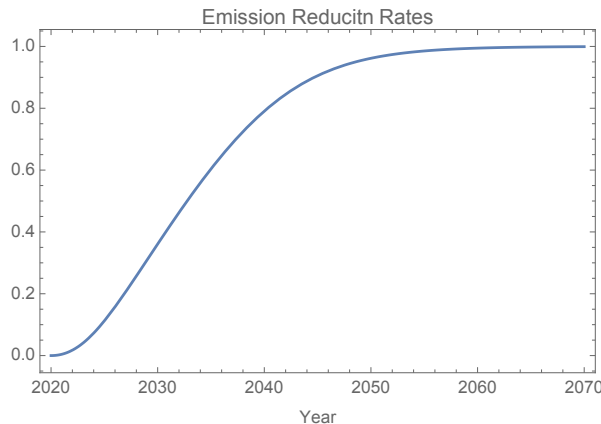


Figure 3: Emission reduction rates, relative to “No-New-Policy”, for the Global Green Deal

The next question is how should we distribute the reduction burden among the sixteen regions? The answer is provided by a basic economic intuition: we should aim for the distribution such that all regions' carbon prices, i.e., the marginal costs of emission reduction, are equalized. Otherwise, it would be mutually beneficial for a pair of regions to arrange a bilateral deal to shift some reduction burden to the region with lower carbon price in exchange for monetary payment from the region with higher carbon price. In other words, any distribution that fails to equalize carbon prices will not be Pareto efficient. In our model, the carbon price can be calculated by:

$$\text{Carbon price}_i = \frac{\partial Y_i(t)}{\partial E_i(t)} = \frac{\partial Y_i(t)/\partial a_i(t)}{\partial E_i(t)/\partial a_i(t)} = \frac{\beta_1 \beta_2}{\hat{\sigma}_{\text{USA},2005}} \cdot a_i(t)^{\beta_2 - 1} \cdot \frac{Y_i(t)}{\hat{Y}_{i,t}}$$

Since the actual output $Y_i(t)$ is only slightly different from the “No-New-Policy” output $\hat{Y}_i(t)$, applying the same emission reduction rates across regions will approximately equalize the carbon prices¹⁸. Hence, we propose that each region should adopt the same emission reduction policy as that in the European Green Deal. It is worth reminding that each region's emission reduction rate $a_i(t)$ in our model is relative to its own “No-New-Policy” emission $\hat{E}_{i,t}$ instead of its 2020 level \hat{E}_{i,t_0} . Figure 4 shows the EU and China's carbon emission, for example, in the Global Green Deal.

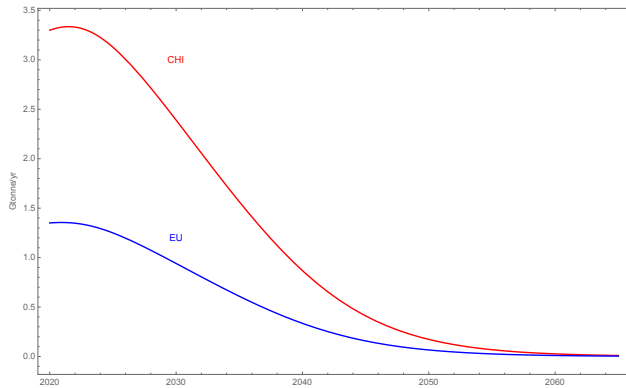


Figure 4: Extrapolated carbon emission for the EU and China in the Global Green Deal

¹⁸Carbon price can also be defined in terms of social welfare. Under this definition, a region with higher per capita consumption should be assigned higher reduction rate. However, equalizing carbon price in this case may not be Pareto efficient unless direct welfare transfer is possible.

3.2 Impacts on Climate and Social Welfare

Based on the estimation, global CO₂ emission under the “No-New-Policy” scenario will gradually approach the peak level near the beginning of next century. The atmospheric CO₂ concentration rises sharply during this period and will reach 762 parts per million (ppm) by the end of this century¹⁹. Meanwhile, global average temperature will increase by 3.5 °C and keeps rising. We can see in Figure 5 that the Global Green Deal can limit global temperature increase just below 2 °C as targeted by the Paris Agreement. As a comparison, if we postpone achieving net-zero emission till the end of this century, then global temperature increase will be stabilized at around 2.7 °C instead.

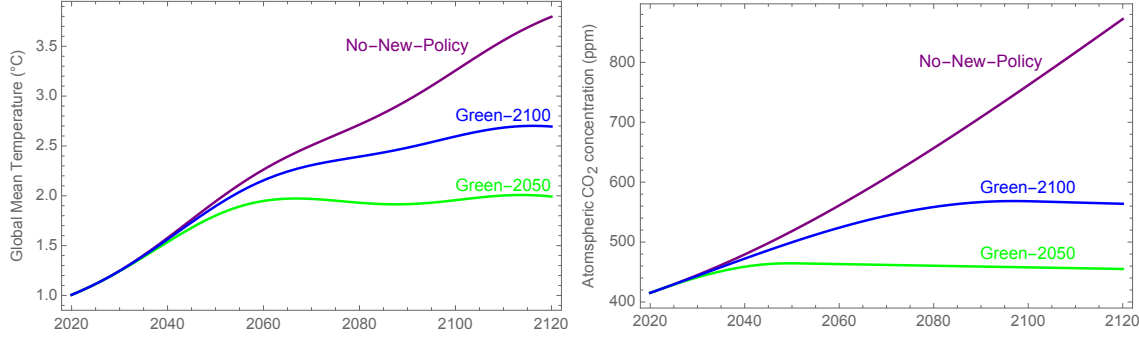


Figure 5: Projected global temperature increase (left) and atmospheric CO₂ concentration (right) under “No-New-Policy” Scenario (purple), net-zero emission by 2050 (green) and net-zero emission by 2100 (blue).

We next examine the economic incentives for the Global Green Deal. Figure 6 shows that although halting further progress when the emission reduction rate reaches 0.9 and maintaining it at that level thereafter yields slightly less global welfare loss, achieving net-zero emission by mid-century is still justifiable from the global perspective: compared to that in the “No-New-Policy” scenario, the Global Green Deal can reduce global welfare loss by 35%, accounting for the emission reduction costs.

However, by examining the sixteen regions’ social welfare individually, we find that benefit of this global effort is not evenly distributed. We can see in Table 4 that impacts on the social welfare, under the “No-New-Policy” scenario, are much higher for the less developed regions. This is because these regions’ economic production relies more on agriculture and other natural resources, thus is more vulnerable to climate change. In addition, it is difficult for these regions to adapt to climate

¹⁹The current level of atmospheric CO₂ concentration is about 415 ppm.

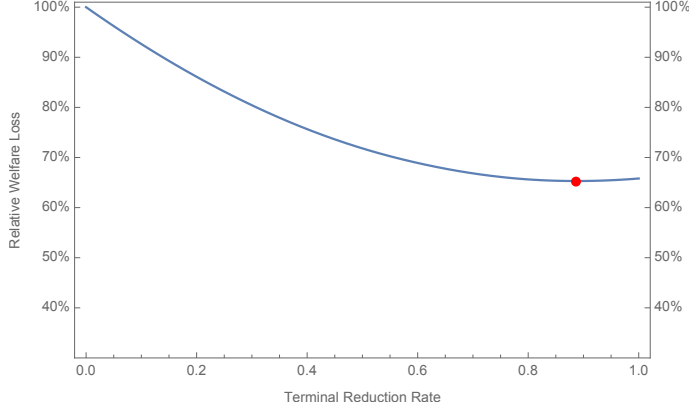


Figure 6: Relative global welfare losses of that in the “No-New-Policy” scenario under different terminal rates for the Global Green Deal (blue line). The terminal reduction rate indicates when the emission reduction rate stops increasing and the reduction level being maintained thereafter. The maximum global welfare is achieved when emission reduction terminates at 0.88(red dot).

change since direct mitigations are more expensive for them²⁰. For same reasons, we can see in Table 4 that benefit of the Global Green Deal leans heavily towards the developing regions.

Table 4: Social welfare loss: No-New-Policy versus Global Green Deal

	No-New-Policy	Global Green Deal	No-New-Policy	Global Green Deal
United States	0.08%	0.44%	Central America	0.30%
Canada	0.07%	0.84%	South America	0.27%
Western Europe	0.18%	0.52%	South Asia	0.26%
Japan and South Korea	-0.03%	0.22%	Southeast Asia	0.45%
Australia and New Zealand	-0.02%	0.54%	China Plus	0.20%
Central and Eastern Europe	0.09%	2.33%	North Africa	2.71%
Former Soviet Union	0.27%	1.17%	Sub-Saharan Africa	3.73%
Middle East	0.30%	0.47%	Small Island States	0.34%
Global	1.09%	0.72%		0.24%

Note: The social welfare losses are measured as fractions of those from the background economy. Japan and South Korea (JPK) and Australia and New Zealand (ANZ) have higher social welfare under “No-New-Policy” scenario than that of the background economy, and hence the corresponding social welfare losses are negative.

On the other hand, Table 4 also suggests that the Global Green Deal can hardly be justified for the developed regions. For this, we have two comments. The first is that although we measure benefits of improved climate by economic terms whenever possible, there are benefits that are difficult to be measured by this way and thus are not accounted for in the model. The developed regions would have more reason to support the Global Green Deal if those benefits were included. Secondly, all the studies we used in estimating the climate change impacts are based on scenarios

²⁰For example, increase in global temperature may increase the mortality and morbidity rate of diarrhea. While it is easy for the developed regions to directly mitigate this impact, the same can not be said for the less developed regions.

with moderate increase in global temperature. It is difficult to tell what would really happen if temperature increase exceeds 3 °C. In other words, we have much less uncertainty regarding the social welfare impacts of the Global Green Deal compared to those in the “No-New-Policy” scenario. Therefore, it can be preferable to support the Global Green Deal even for the developed regions for avoiding the otherwise large uncertainty.

From these results, we can conclude that a Global Green Deal for achieving net-zero CO₂ emission by mid-century is necessary for meeting the goal set by the Paris Agreement: any delay would make global temperature increase go beyond 2 °C before this century ends. This global effort reduces global welfare loss by 35% and it is particularly beneficial for most developing regions.

4 Cooperation and Trigger Strategies

We now investigate whether cooperation on the Global Green Deal, despite of free-riding incentives, can be sustained by using trigger strategies. The problem of free-riding exists in any public-good provision due to the positive externality. Specifically in our context, each region pays the full cost of emission reduction while the benefit of it is shared by all regions. This positive externality leads to free-riding incentives: each region prefers to benefit from other regions’ emission reduction efforts without contributing its own fair share. As a result, a region may (1) withdraw from the Global Green Deal when cooperation is not supported by a binding agreement, or (2) not participate at all when it expects to be confined by a binding agreement. Although trigger strategies are often used to deter free-riding incentives in the first scenario, the main idea can also be applied in the latter one. In this section, we examine whether trigger strategies are effective in supporting the Global Green Deal under these two scenarios, respectively.

4.1 Cooperation without Binding Agreement

If the sixteen regions cannot enforce a binding agreement for the Global Green Deal, then the cooperation may fail if one or more regions choose to withdraw or defect from it due to the free-riding incentives. In game theory, one approach to overcome this problem is to use trigger strategies. Formally speaking, a strategy s_i for region i is defined as a complete contingent plan. It prescribes an emission reduction rate $s_i(a^t)$ at time t given the observed reduction rates of all regions before

then. A trigger strategy is a special type of strategy that in general takes the following form:

$$s_i(a^t) = \begin{cases} \hat{a}(t) & , \text{ if } a^t = (\hat{a}_j(k))_{j,k < t}; \\ \tilde{s}_i(a^t) & , \text{ otherwise.} \end{cases}$$

We can interpret the collection of emission reduction rates $(\hat{a}_i)_{i,t \geq t_0}$ as the targeted cooperative outcome and the embedded strategies $(\tilde{s}_i)_i$ as contingent punishment plans. Using trigger strategies by all regions implies that each region will keep implementing the targeted policy as long as all regions have been implementing it before then, but the punishment phase will be triggered when defection occurs. The idea is for the embedded strategies $(\tilde{s}_i)_i$ to lead to a sufficiently bad outcome so that unilateral defection is deterred and cooperation is sustained.

Most studies²¹ on trigger strategies in the context of international climate cooperation focus on the so-called grim trigger strategies in which all participants immediately switch back to the “business-as-usual” indefinitely once defection of any kind occurs. As emphasized in [Mason et al. \(2017\)](#), this type of trigger strategy is not robust against renegotiation: the embedded punishment loses its credibility since starting a new agreement is beneficial for all countries. We therefore start with a more realistic benchmark trigger strategy in which defection immediately triggers all other regions to switch to the same emission reduction policy as that of the defecting region. With this type of trigger strategy, severeness of the punishment increases with the degree of defection and cooperation by all regions resumes if the defecting region cooperates again.

We begin with the scenario in which a defecting region simply withdraw from the Global Green Deal without rolling back its achieved progress. Table 5 shows that this benchmark trigger strategy is not effective in sustaining cooperation on the Global Green Deal. Most regions, except for the two African regions, will halt further progress before reaching net-zero carbon emission even when other regions are cooperating.

Table 5 also shows that the benchmark trigger strategy tends to be more effective in deterring defection for the regions who suffer more from climate change. This result demonstrates an important limitation of using trigger strategies to sustain climate cooperation. The general and essential idea of trigger strategies in this context is to use a worse climate, due to less ambitious emission

²¹See for example [Dockner et al. \(1996\)](#), [Dutta and Radner \(2009\)](#) and [Dutta and Radner \(2010\)](#).

Table 5: Defection without rollback under benchmark trigger strategy

Defect when reduction rate reaches:		Defect when reduction rate reaches:	
United States	0.1	Central America	0.5
Canada	0.1	South America	0.7
Western Europe	0.2	South Asia	0.4
Japan and South Korea	0.1	Southeast Asia	0.7
Australia and New Zealand	0.0	China Plus	0.5
Central and Eastern Europe	0.1	North Africa	1.0
Former Soviet Union	0.3	Sub-Saharan Africa	1.0
Middle East	0.3	Small Island States	0.8

Note: The results are from simulations. The number for each region shows when it will withdraw from the Global Green Deal assuming all other regions are cooperating before then.

reduction from the punishing regions, as a threat in order to deter potential defection. However, regions with less economic incentives to cooperate are often those that are less vulnerable to climate change. This creates a situation in which the threat imposed by trigger strategies tends to be less severe for those that are more likely to defect. This situation compromises the effectiveness of trigger strategies. We can see in Table 5 that the benchmark trigger strategy quickly loses its effectiveness when the Global Green Deal barely starts²².

This result is robust even under more severe punishment. To demonstrate this point, we consider an alternative trigger strategy in which defection of any kind will immediately trigger all other regions to roll back their progresses by decreasing the emission reduction rate by 0.05 per year until it reaches zero. This trigger strategy is more similar to the one that uses “business-as-usual” as threat against defection. Taking the United States as an example, Table 6 shows that it still does not have incentive to delay the defection. In fact, this unconditional ‘rollback’ trigger strategy will induce the United States to also roll back its own progress in contrast to the benchmark trigger strategy for which the better option for the United States is to simply withdraw from cooperation without rolling back its progress.

Table 6: Relative social welfare losses for the United States under different trigger strategies.

	U.S. withdraws at 0.1	U.S. withdraws at 0.2	U.S. withdraws at 0.1 with rollback
Benchmark trigger strategy	89.07%	89.48%	99.51%
Rollback trigger strategy	100.54%	110.88%	99.51%

Note: The percentage terms are the relative social welfare loss for the United States compared to that in the “No-New-Policy” scenario.

²²For practical purpose, each region is only allowed to defect when the emission reduction rate reaches $0.1 * n$ for $n = 1, 2, \dots, 10$ in the simulation. Under a finer increment, Australia and New Zealand region will defect when the emission reduction rate is slightly above zero

In view of the ineffectiveness in sustaining global cooperation, we next investigate whether trigger strategy is more effective in sustaining cooperation among smaller sets of regions. More specifically, we consider the case in which the benchmark trigger strategies are adopted only among a subset \mathcal{S} of regions such that cooperation continues if and only if all regions in \mathcal{S} have been implementing the Green Deal. We begin by first excluding the Australia and New Zealand region who would almost immediately withdraw from the global cooperation. Table 7 shows that cooperation of the remaining regions can only be sustained until the emission reduction rate reaches 0.1 by the benchmark trigger strategy, after which four other developed regions²³ will withdraw from cooperation. As we move down the list in Table 7, the remaining regions have increasingly more similar climate change impacts. However, we can see from Table 7 that reducing heterogeneity in climate change impacts by including less regions does not significantly improve the outcome. The reason is that including less regions in the cooperation reduces the effect on the global carbon emissions and hence reduce the effect on global climate. Therefore, the degree of deterrence, measured by the social welfare difference between that in the targeted outcome and that in the punishment phase, shrinks as well as we exclude increasingly more regions. We can clearly see this point from the last row of Table 7. In this case, the remaining regions²⁴ are those who suffer most from climate change. However, since their total carbon emission is only about a quarter of the global emission, it is not sufficient for the trigger strategy to create meaningful deterrence. Consequently, defection occurs almost immediately.

Table 7: Regional cooperation under benchmark trigger strategy

Excluding	Fraction of global emission	Cooperation sustained until reduction rate reaches:	Relative global welfare loss
ANZ	98%	0.10	92.75%
USA, CAN, JPK, CEE	80%	0.10	94.94%
WEU	68%	0.20	92.06%
FSU, MDE	61%	0.25	92.43%
SAS	55%	0.20	94.79%
CHI	26%	0.00	100.00%

Note: The first column shows the regions that are excluded from the previous regional cooperation. The second column are total fractions of global carbon emission for the remaining regions at the reference year 2020. The third column shows when the regional cooperation stops. The last column are achieved relative global welfare loss compared to that of the “No-New-Policy” scenario.

From these results, we can conclude that when the Global Green Deal is not supported by a binding agreement, trigger strategies are not effective in deterring defection. The reason is that

²³United States, Canada, Japan and South Korean, and Central and Eastern Europe.

²⁴Central America, South America, Southeast Asia, North Africa, Sub-Saharan Africa and Small Island States.

the potential punishments in trigger strategies rely on creating a worse climate compared to that of the Global Green Deal, but this type of threat is less effective against defection of the developed regions as those regions tend to suffer less from climate change at the first place. The best outcome that can be achieved in this scenario is for all developing regions to seek cooperation with a less ambitious goal among themselves as shown in the third row of Table 7. This outcome is only slightly better than that in the “No-New-Policy” scenario, in terms of global welfare.

4.2 Binding Agreement and “All-or-Nothing” Approach

We now examine the scenario in which the sixteen regions are able to enforce a binding agreement to support cooperation. Although we have seen examples, in the real world, of withdrawing from an international agreement, it is also true that such action may partially be deterred for non-economic reasons. Therefore, studying cooperation under a binding agreement is still relevant. On the other hand, a fundamental requirement for any international agreement is that it must respect sovereignty of the countries or regions. In other words, countries cannot be forced to sign the agreement if it is not in their best interests to do so, due to the free-riding incentives for example. Although trigger strategies cannot formally be applied for this scenario, the main idea remains in the form of an “all-or-nothing” agreement: every region agrees that the agreement is in effect if and only if all regions have signed it.

To demonstrate why a region may choose to not sign a potentially beneficial agreement and why the “all-or-nothing” agreement may be useful and necessary, we use an example in which cooperation starts with the Asian and African regions together with Small Island States. For this subset of regions, we find that the “all-or-nothing” approach can support an agreement in which the target is to implement the Green Deal until the emission reduction rate reaches 0.4. By comparing the relative social welfare loss for Central American and South American in the second and the third column in Table 8, we can see that these two regions will not join the cooperation since free-riding allows them to have lower social welfare loss. However, if the cooperation is conditional on their participation, then they will sign the agreement to also partially implement the Green Deal, since they would otherwise lead the world to the “No-New-Policy” scenario in which they will have higher social welfare losses. This example demonstrates that the “all-or-nothing” approach can encourage participation, but the cooperation must be beneficial to all participating regions

compared to the “No-New-Policy” scenario.

Table 8: Relative welfare losses under agreements that partially implement the Green Deal plan

Agreements	\mathcal{S}^0 (0.40)	\mathcal{S}^1 (0.40)
Central America’s relative social welfare loss:	81.6%	93.1%
South America’s relative social welfare loss:	86.2%	91.8%

Note: The percentage terms are relative social welfare loss compared to that in the “No-New-Policy” scenario. $\mathcal{S}^0 = \{\text{SAS, SEA, CHI, NAF, SSA, SSI}\}$ and $\mathcal{S}^1 = \mathcal{S}^0 + \{\text{CAM, SAM}\}$.

As we have already seen in section 3.2, the Global Green Deal does not benefit the developed regions, and therefore it can not be sustained even when a binding agreement is available and the “all-or-nothing” approach is applied. Based on simulations, we find that the best outcome that can be achieved in this scenario is for the agreement to assign different and less ambitious emission reduction targets across regions instead of insisting on net-zero emission. As shown in Table 9, this second-best cooperation agreement reduces the global welfare loss to 76.4% of that in the “No-New-Policy” scenario.

Table 9: Emission reduction targets in the “second-best” Global Green Deal

Emission reduction target		Emission reduction target	
United States	0.3	Central America	0.6
Canada	0.1	South America	0.6
Western Europe	0.3	South Asia	0.6
Japan and South Korea	0.1	Southeast Asia	0.6
Australia and New Zealand	0.0	China Plus	0.6
Central and Eastern Europe	0.1	North Africa	0.6
Former Soviet Union	0.4	Sub-Saharan Africa	0.6
Middle East	0.5	Small Island States	0.6
Relative global welfare loss	76.4%		

Note: The relative global welfare loss is calculated by comparing to that in the “No-New-Policy” scenario.

Although this cooperation outcome can achieve a higher global welfare compared to that in the first scenario, it relies on two strong assumptions: (1) a binding agreement is plausible, and (2) all regions can agree to continue with the “No-New-Policy” emission if one or more regions do not sign the agreement. In addition, the agreement for this cooperation assigns much less ambitious emission reduction targets for the developed regions, for which it may be politically controversial to advocate. Nonetheless, it provides us with a ‘best-case-scenario’ that shows what could possibly

be achieved using the idea of trigger strategies.

5 Transfer Payments

We now address the last question: can transfer payments support the Global Green Deal? The answer to this question is clearly ‘yes’, if direct welfare transfer is possible and if the sixteen regions can enforce a binding agreement: since the global welfare, as the sum of the sixteen regions’ social welfare, is higher than that in the “No-New-Policy” scenario, we can always find a collection of welfare transfers such that all regions will prefer to participate in the Global Green Deal. In this section, we investigate whether we will have the same answer when (1) transfer payments must be in monetary terms and (2) binding agreement is not plausible, respectively.

We first characterize the required monetary payments assuming binding agreement is still available. In particular, we use $m_{i,t}$ to represent the net monetary payment received for region i at time t . To simplify the discussion, we assume that these payments will not affect each region’s consumption-investment decision so that each region i ’s consumption at time t becomes:

$$\tilde{C}_i(t) = C_i^*(t) + m_{i,t}, \quad (16)$$

where C_i^* is the solution to the optimization problem (5), and is determined by the sixteen regions’ emission reduction policies.

Suppose we include monetary payments in a binding agreement to support the Global Green Deal and the alternative is the “No-New-Policy” outcome, then each region i would be willing to participate if and only if:

$$\int_{t_0}^{\infty} P_{i,t} \frac{(\hat{C}_i(t)/P_{i,t})^{1-\theta}}{1-\theta} e^{-\rho(t-t_0)} dt \leq \int_{t_0}^{\infty} P_{i,t} \frac{((C_i^{\text{GGD}}(t) + m_{i,t})/P_{i,t})^{1-\theta}}{1-\theta} e^{-\rho(t-t_0)} dt. \quad (17)$$

where \hat{C}_i and C_i^{GGD} are consumption in the “No-New-Policy” scenario and in the Global Green Deal, respectively. Notice that the social welfare for the Global Green Deal with transfers, or the right-hand-side of the above condition, is continuous with respect to the net payments received $(m_{i,t})_{t \geq t_0}$. Therefore, we only need to consider the case in which each region receives the same net monetary transfer across time, i.e., $m_{i,t} \equiv \bar{m}_i$.

Table 10: Minimum net monetary transfer (Billions of 2020\$) required for participation

	Global Green Deal	70% Green Deal		Global Green Deal	70% Green Deal
United States	152.9	183.8	Central America	1.6	-8.3
Canada	28.1	33.4	South America	-20.3	-24.7
Western Europe	83.3	103.7	South Asia	19.0	-25.3
Japan and South Korea	24.0	28.7	Southeast Asia	-55.1	-66.8
Australia and New Zealand	20.0	23.3	China Plus	-11.3	-126.4
Central and Eastern Europe	93.1	109.2	North Africa	-138.1	-112.8
Former Soviet Union	36.6	49.7	Sub-Saharan Africa	-242.1	-189.4
Middle East	11.6	19.3	Small Island States	-2.7	-2.9
Global total	696.9	-106.9			

Note: Monetary payments are measured by billions of purchasing-power-parity adjusted US dollars in 2020.

The first column for each region in Table 10 shows the minimum net transfer payments required for each region to be willing to participate in the Global Green Deal, and the negative numbers can be interpreted as the maximal amounts of money those region would be willing to pay for the Global Green Deal. We can see in Table 10 that the world will need an average of 696.9 billions of dollars per year to support the Global Green Deal. If there is no external funding and thus the global budget of the agreement cannot be in deficit, then the best outcome that can be sustained is for all regions to implement the Green Deal until the emission reduction rate reaches 0.7, based on simulations. The second column for each region in Table 10 shows the required net transfer payments in this case.

We now discuss why a binding agreement is necessary. When monetary transfers can be enforced through a binding agreement, how they are distributed across time will not affect each region's incentive for participation. However, for the cooperation on emission reduction, the benefits of improved climate are distributed across a long-period of time due to the long-last impact of CO₂ emission on the climate, but the costs of emission reduction must be paid immediately. This suggests that there may be budget imbalance at the early stage of cooperation. Consequently, it requires that either some regions are willing to postpone receiving the payments, or some regions are willing to temporarily pay more than the realized benefit from cooperation. As shown in Figure 7, cooperation on the Green Deal until emission reduction reaches 0.7 will create a long period of time where the benefit of cooperation, in terms of consumption, is lower than the total net transfer payment. Without a binding agreement to enforce transfer payments, it would be difficult for any regions to postpone receiving or temporally increase payments for more than four decades, as suggested by Figure 7. Therefore, although transfer payments can achieve the best cooperation

outcome so far, both in terms of global welfare and in terms of the global climate as shown in Figure 8, a binding agreement to enforce payments is likely required.

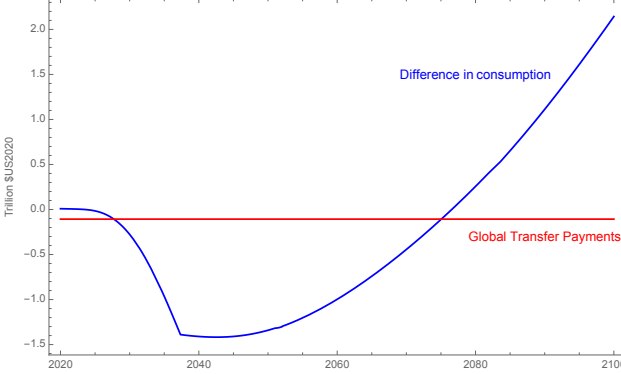


Figure 7: Difference in consumption between “No-New-Policy” and 70% Green Deal vs. required transfer payments.

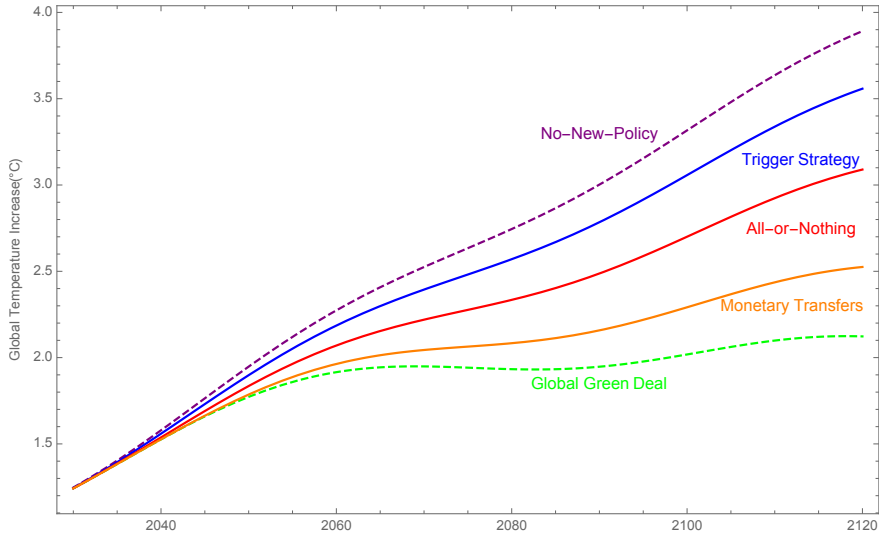


Figure 8: Global mean temperature increase under “No-New-Policy” scenario (purple dashed line), cooperation among developing regions sustained by trigger strategies (blue line), global cooperation with binding agreements and “all-or-nothing” approach (red line), global cooperation sustained by monetary transfers (orange line), and the Global Green Deal (green dashed line).

6 Conclusion

Through the study of international cooperation on emission reduction, we find that the global cooperation on achieving net-zero CO₂ emission by mid-century is worth pursuing as a global target. It cuts the global welfare loss by 35%, accounting for the emission reduction cost. However, this

cooperation is vulnerable to the free-riding incentives and we find that trigger strategies are not very effective in sustaining cooperation. Transfer payments among the sixteen regions can help improve the cooperation outcome, but they are not able to support global net-zero carbon emission by mid-century. Relying on numerical methods and simulations may have restricted our scope of analysis, but it allows us to use an integrated climate-economic model based on empirical studies to obtain insights that cannot be obtained from a more stylized game-theoretic model. In particular, our analysis has revealed an important obstacle for international climate cooperation: climate change impacts are highly heterogenous across regions. Combined with free-riding incentives, it makes the trigger strategies less effective than what is suggested in previous work on this topic. Our study also suggests that the goal of the Paris Agreement for limiting global temperature increase under 2 °C is difficult to be accomplished through cooperation on emission reduction. Alternative methods and techniques for controlling the climate may be necessary, especially for economically less developed regions.

References

- D. Acemoglu, U. Akcigit, D. Hanley, and W. Kerr. “Transition to Clean Technology”. *Journal of Political Economy*, 124(1):52–104, 2016.
- D. Anthoff and R. S. Tol. “*The Climate Framework for Uncertainty, Negotiation and Distribution (FUND), Technical Description, Version 3.9*”, 2014.
- J. Bao, W.-H. Lu, J. Zhao, and X. Bi. “Greenhouses for CO₂ Sequestration from Atmosphere”. *Carbon Resources Conversion*, 1:183–190, 2018.
- L. M. Brander, K. Rehdanz, R. S. Tol, and P. J. van Beukering. “The Economic Impact of Ocean Acidification on Coral Reefs”. *Climate Change Economics*, 3(1):1–29, 2012.
- D. Cass. “Optimum Growth in an Aggregative Model of Capital Accumulation”. *The Review of Economic Studies*, 32(3):233–240, 1965.
- N. Chen, C. Ding, C. Singer, and B. Yang. “Global and Regional Extrapolations of CO₂ Emissions: With an Example of Possible Security Benefits to Western Europe of Reduced Fossil Fuel Imports”. Report, prepartation in progress, University of Illinois at Urbana-Champaign Program in Arms Control & Domestic and International Security, 2020.
- C. Ding. “Global Heat Balance without and with Solar Radiation Management”. Master’s thesis, University of Illinois at Urbana-Champaign, 2018.
- E. J. Dockner, N. V. Long, and G. Sorger. “Analysis of Nash Equilibria in a Class of Capital Accumulation Games”. *Journal of Economic Dynamics and Control*, 20:1209–1235, 1996.

- P. K. Dutta and R. Radner. "A Strategic Analysis of Global Warming: Theory and Some Numbers". *Journal of Economic Behavior & Organization*, 71:187 – 209, 2009.
- P. K. Dutta and R. Radner. "Capital Growth in a Global Warming Model: Will China and India Sign a Climate Treaty?". *Economic Theory*, 49:411–443, 2010.
- GBD 2016 Diarrhoeal Disease Collaborators. "Estimates of the Global, Regional, and National Morbidity, Mortality, and Aetiologies of Diarrhoea in 195 Countries: A Systematic Analysis for the Global Burden of Disease Study 2016". *The Lancet*, 18(11):1211–1228, 2018.
- K. Gillingham and J. H. Stock. "The Cost of Reducing Greenhouse Gas Emissions". *Journal of Economic Perspectives*, 32(4):53–72, 2018.
- K. Gillingham, W. Nordhaus, D. Anthoff, G. Blanford, V. Bosetti, P. Christensen, H. McJeon, and J. Reilly. "Modeling Uncertainty in Integrated Assessment of Climate Change: A Multimodel Comparison". *Journal of the Association of Environmental and Resource Economists*, 5(4):791–826, 2018.
- A. Grinsted, J. Moore, and S. Jevrejeva. "Reconstructing Sea Level from Paleo and Projected Temperatures 200 - 2100 AD". *Climate Dynamics*, 34:461–472, 2010.
- B. Harstad. "Climate Contracts: A Game of Emissions, Investments, Negotiations, and Renegotiations". *The Review of Economic Studies*, 79(4):1527–1555, 2012.
- T. Koopmans. "On the Concept of Optimal Economic Growth". Cowles Foundation Discussion Papers 163, Cowles Foundation for Research in Economics, Yale University, 1963.
- N. Lenssen, G. Schmidt, J. Hansen, M. Menne, A. Persin, R. Ruedy, and D. Zyss. "Improvements in the GISTEMP uncertainty model". *Journal of Geophysical Research Atmospheres*, 124(12): 6307–6326, 2019.
- M. Marilena, G. Diego, S. Edwin, C. Monica, S. Efisio, O. Jos, and V. Elisabetta. "Fossil CO₂ Emissions of All World Countries - 2018 Report". Publications Office of the European Union, 2018.
- C. F. Mason, S. Polasky, and N. Tarui. "Cooperation on Climate-Change Mitigation". *European Economic Review*, 99:43–55, 2017.
- T. Milligan. "Development of an Econo-Energy Model and an Introduction to a Carbon and Climate Model for Use in Nuclear Energy Analysis". Master's thesis, University of Illinois at Urbana-Champaign, 2012.
- W. Nordhaus and P. Sztorc. "DICE 2013R: Introduction and User's Manual", second edition edition, October 2013.
- W. D. Nordhaus. "Economic Aspects of Global Warming in a Post-Copenhagen Environment". *Proceedings of the National Academy of Sciences*, 107(26):11721–11726, 2010.
- W. D. Nordhaus. "Integrated Economic and Climate Modeling". In P. B. Dixon and D. W. Jorgenson, editors, *Handbook of Computable General Equilibrium Modeling*, volume 1, pages 1069–1131. New York: Elsevier, 2013.
- W. D. Nordhaus and Z. Yang. "A Regional Dynamic General-Equilibrium Model of Alternative Climate-Change Strategies". *American Economic Review*, 86(4):741–765, 1996.

- W. H. Press, B. P. Flannery, S. A. Teukolsky, and W. T. Vetterling. “*Numerical Recipes in FORTRAN: The Art of Scientific Computing*”, chapter 16, pages 704–716. Cambridge University Press, 1992.
- F. P. Ramsey. “A Mathematical Theory of Saving”. *The Economic Journal*, 38(152):543–559, 1928.
- K. Riahi, D. P. van Vuuren, E. Kriegler, J. Edmonds, B. C. O’Neill, S. Fujimori, N. Bauer, K. Calvin, R. Dellink, O. Fricko, W. Lutz, A. Popp, J. C. Cuaresma, S. KC, M. Leimbach, L. Jiang, T. Kram, S. Rao, J. Emmerling, K. Ebi, T. Hasegawa, P. Havlik, F. Humpenöder, L. A. D. Silva, S. Smith, E. Stehfest, V. Bosetti, J. Eom, D. Gernaat, T. Masui, J. Rogelj, J. Strefler, L. Drouet, V. Krey, G. Luderer, M. Harmsen, K. Takahashi, L. Baumstark, J. C. Doelman, M. Kainuma, Z. Klimont, G. Marangoni, H. Lotze-Campen, M. Obersteiner, A. Tabeau, and M. Tavoni. The shared socioeconomic pathways and their energy, land use, and greenhouse gas emissions implications: An overview. *Global Environmental Change*, 42:153–168, jan 2017. doi: 10.1016/j.gloenvcha.2016.05.009.
- H. Rogner. “An Assessment of World Hydrocarbon Resources”. *Annual Review of Energy and The Environment*, 22:217–262, 1997.
- C. Singer and L. Matchett. “Climate Action Gaming Experiment: Methods and Example Results”. *Challenges*, 6:202–228, 2015.
- C. Singer, T. Rethinraj, S. Addy, D. Durham, M. Isik, M. Khanna, B. Keuhl, J. Luo, W. Quimo, and R. Kothavari. “Probability Distribution for Carbon Emissions and Atmospheric Response”. *Climate Change*, 88:309–342, 2008.
- C. Singer, T. Milligan, and T. Rethinraj. “How China’s Options will Determine Global Warming”. *Challenges*, 5:1–25, 2014.
- E. A. Stanton, F. Ackerman, and S. Kartha. “Inside the Integrated Assessment Models: Four Issues in Climate Economics”. *Climate and Development*, 1(2), 2009.
- N. Tauchnitz. “The Pontryagin Maximum Principle for Nonlinear Optimal Control Problems with Infinite Horizon”. *Journal of Optimization Theory and Applications*, 167:27–48, 2015.
- R. S. Tol. “The Economic Impacts of Climate Change”. *Review of Environmental Economics and Policy*, 12(1):4–25, 2018.

Appendices

A Geographic Regions

Table A1: List of countries in the sixteen geographic regions.

Region	Name	ISO															
USA	United States	ASM GUM MNP USA															
CAN	Canada	CAN															
WEU	Western Europe	AND AUT BEL CYM CHA CYP DNK FLK FRO FIN FRA DEU GIB GRC GRL VAT ITA IMN LIE LUX MLT MCO MSR NLD PRT SHN MAF SMR ESP CHE TCA GBR WLF															
JPK	Japan and South Korea	JPN KOR															
ANZ	Australia and New Zealand	AUS COK NZL NIU TKL															
CEE	Central and Eastern Europe	ALB BIH BGR HRV CZE HUN MKD MNE POL SRB SVK SVN															
FSU	Former Soviet Union	ARM AZE BLR EST GEO KAZ KGZ LVA LTU MDA RUS TJK															
MDE	Middle East	BHR IRN IRQ ISR JOR KWT LBN OMN PSE QAT SAU SYR															
CAM	Central America	BLZ CRI SLV GTM HND MEX NIC PAN															
SAM	South America	ARG BOL BRA CHL COL ECU GUY PRY PER SUR URY VEN															
SAS	South Asia	AFG BGD BTN IND PAK LKA															
SEA	Southeast Asia	BRN KHM IDN LAO MYS MMR PNG PHL SGP THA TLS VNM															
CHI	China Plus	CHN PRK MNG															
NAF	North Africa	DZA EGY LBY MAR TUN ESH															
SSA	Sub-Saharan Africa	AGO BEN BWA BFA BDI CMR CPV CAF TCD COG COD CIV DJI GNQ ERI ETH GAB GAB GMB GHA GIN GNB KEN LSO LBR MDG MWI MLI MRT MOZ NAM NER NGA RWA SEN ZAF SSD SDN SWZ TZG TGO UGA ZMB ZWE															
SIS	Small Island States	AIA ATG ABW BHS BRB BMU BES VGB COM CUB CUW DMA DJI GNQ ERI ETH GAB GAB GMB GHA GIN GNB KEN DOM FJI PYF GRD GRD GLP HTI JAM KIR MHL MUS FSM NRU NCL PLW PRI REU BLM KNA LCA VCT WSM STP SYC SXM SLB TON TTO TUV VUT VIR															

Note: Countries and other UN reporting units are represented by the International Standards Organization (ISO) code: <https://www.iso.org/publication/PUB500001.html>, accessed December 15, 2019.

B Extrapolation of Exogenous Variables

B.1 “No-New-Policy” Carbon Emissions

The carbon emissions are measured in GtonneC/yr. The global carbon emissions are divided into those from land use changes and those from industry.

$$\hat{E}_t = \hat{E}_{land,t} + \hat{E}_{industry,t}.$$

The carbon emissions from land-use change is fit with the function below:

$$\hat{E}_{land,t} = b_{11} \frac{1}{1 + e^{-(t-b_{12})/b_{13}}} \left(1 - \frac{1}{1 + e^{-(t-b_{12})/b_{13}}} \right) + \frac{b_{21}}{\sqrt{2\pi}} e^{-(1/2((t-b_{22})/b_{23})^2)}.$$

The first term is the first-order derivative of the logistic function with respect to time that represents the long term trend of emission from land use change. The second term accounts for the observed short-term surge centered around 1993. The industrial carbon emissions are extrapolated using:

$$\hat{E}_{industry,t} = g_c \times \frac{b_{31}}{1 + e^{-(t-b_{32})/b_{33}}} + f_{p,t} \times \frac{b_{41}}{(1 + e^{-(t-b_{42})/b_{43}})}$$

We divide the industrial emissions into those from the use of coal and those from the fluid fossils. The parameter $g_c = 0.409$ is the historical emission fraction from coal. [Rogner \(1997\)](#) points out that depletion of fluid fossils will increase the associated extraction cost which in turn will decrease the corresponding emissions if emissions follow the current trend. We explore this effect along other lines of our research project. In this paper, however, we assume that $f_{p,t} \equiv 1$ for simplicity and also for the reason that the carbon emissions are controlled by the sixteen regions' reduction policies and thus this depletion effect is unlikely to be significant enough within the time span of our analysis.

Table A2: “No-New-Policy” carbon emission constants and the calibrated values

k	b_{k1} (GtonneC/yr)	b_{k2} (Julian year)	b_{k3} (yr)	Description
1	2.598	2003	162.8	Land use long term trend
2	0.966	1993	15.2	Land us change pulse
3	18.25	2011	29.3	Reference industrial emission
4	11.90	2014	29.4	Industrial fluid fossil

The extrapolation of regional emissions is done by using

$$E_i(t) = fr_i(t) \times E(t),$$

where fr_i is region i 's fraction of global carbon emissions under the “No-New-Policy” scenario. We extrapolate the regional fractions in four steps. In the first step, we divide the sixteen regions into four subgroups: (1) the “Developed” group (USA, CAN, WEU, JPK, ANZ and CEE); (2) CHI; (3) FSU and (4) the “Other” group (SAS, MDE, SEA, CAM, NAF, SAM, SSA, SIS). For each subgroup other than the “Developed”, we use the least-square fit to a group-specific function. The fraction for the “Developed” group is simply derived by

$$fr_{Developed} = 1 - fr_{CHI} - fr_{FSU} - fr_{Other}.$$

Similar exercises are conducted in the remaining three steps. In step two, we extrapolate the regional fractions within the “Developed” group. In step three, we put SAM, SSA, SIS together as the “South” group and extrapolate regional fractions within the “Other” group. In the last step, we extrapolate regional fractions within the “South” group. Figure 9 shows the extrapolated regional fractions of global emissions.

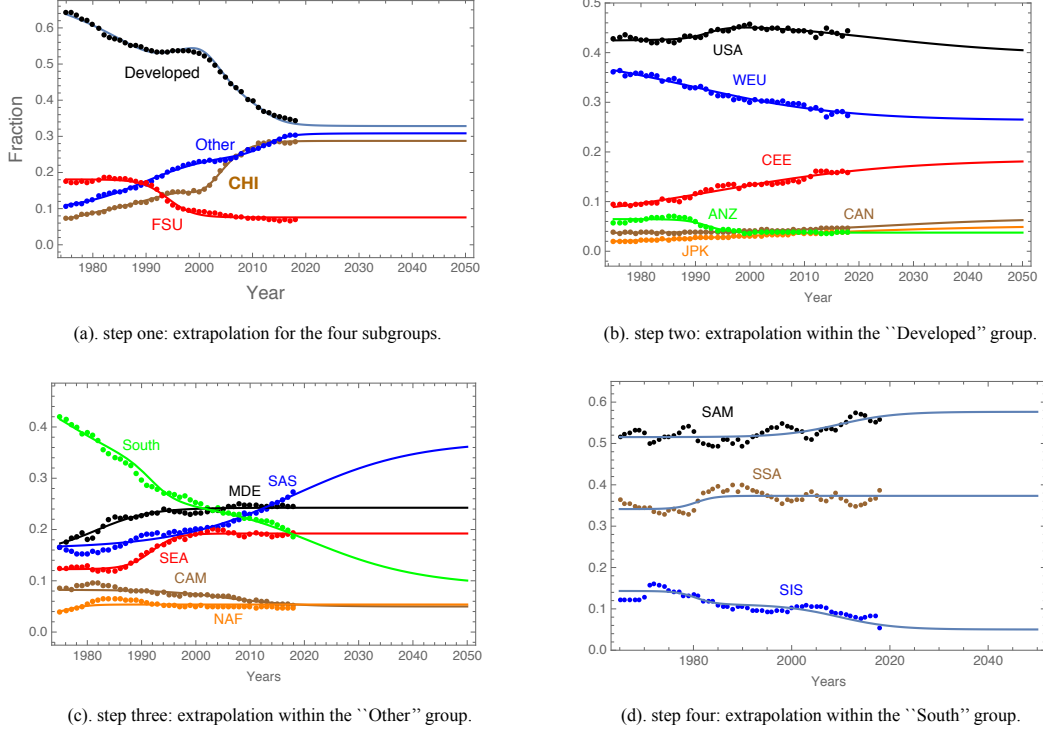


Figure 9: Regional fractions of global CO₂ emissions under ‘‘No-New-Policy’’ scenario are extrapolated using analytic functions in four steps.

B.2 Background Economy

The regional population P_i is divided into subsistence population, denoted by $B_{0,i}$, and the labor inputs. The latter is assumed to be characterized by a logistic function:

$$L_{i,t} = \frac{B_{1,i}}{1 + e^{-(t - B_{2,i})/B_{3,i}}}.$$

These parameters are calibrated using the long-term historical data on population provided by Maddison combined with the projection provided by the United Nations through 2050.

The function form of the background economy’s per capita output is based on [Singer et al. \(2008\)](#) (See Lemma 1):

$$y_{i,t} = b_{0,i} + b_{1,i} \times \left(\frac{A_{i,t}}{\left(1 + \frac{(\rho+r)\theta}{b_{3,i}\omega} (1 - A_{i,t}) \right)^{1-\omega}} \right)^{\frac{1}{\omega}},$$

Table A3: Regional parameter values for the background economy

Symbol	$B_{0,i}$	$B_{1,i}$	$B_{2,i}$	$B_{3,i}$	$b_{0,i}$	$b_{1,i}$	$b_{2,i}$	$b_{3,i}$
Units	Billion	Billion	Julian year	yr	k\$US2020	k\$US2020	Julian year	yr
USA	0.0010	0.4522	1982.04	44.02	3.37	153.87	1998.14	43.37
CAN	0.0008	0.0554	1992.18	39.86	2.97	82.90	1975.32	33.53
WEU	0.1351	0.3234	1937.36	42.13	4.59	64.81	1972.69	25.00
JKP	0.0409	0.1354	1949.36	19.56	1.83	55.08	1975.20	16.85
ANZ	0.0004	0.0534	2010.73	42.80	8.24	93.49	1992.35	31.11
CEE	0.0372	0.0838	1912.67	30.06	2.44	34.41	1972.69	25.00
FSU	0.0537	0.2680	1941.58	36.37	2.41	23.50	1956.21	23.93
MDE	0.0254	0.5195	2008.89	23.72	2.31	42.36	1980.67	31.80
CAM	0.0080	0.2442	1997.62	25.62	2.05	22.84	1961.90	30.50
SAM	0.0099	0.5485	1988.54	27.41	1.60	26.48	1972.23	38.53
SAS	0.2222	2.4358	2002.58	25.36	1.39	67.38	2037.35	17.60
SEA	0.0406	0.9610	1997.18	30.64	1.21	47.62	2016.63	21.10
CHI	0.3947	1.1402	1975.03	17.19	0.80	62.60	2016.54	12.64
NAF	0.0107	0.3977	2022.74	31.18	2.07	31.80	2005.46	41.72
SSA	0.0643	4.9353	2057.89	29.54	1.06	2.89	1955.06	42.35
SIS	0.0045	0.0604	1983.17	30.69	1.62	25.01	1984.56	39.11

Note: k\$US2020 represents one thousand purchasing-power-parity adjusted US dollars in 2020.

and the total productivity is assumed to follow a logistic function:

$$A_{i,t} = \frac{b_{1,i}}{1 + e^{-(t - b_{2,i})/b_{3,i}}}.$$

Since the current climate change impacts are small, we assume that the currently observed data on per capita GDP well-represents the evolution of background economy. Therefore, the parameter values are calibrated using historical data on per capita GDP provided by Maddison and International Monetary Fund.

B.3 “No-New-Policy” Global Temperature

The “No-New-Policy” global mean temperature is fitted with the following analytic function:

$$\hat{\tau}_t = \frac{d_1}{1 + e^{-(t - d_2)/d_3}} + d_4 \cos \frac{2\pi(t - d_5)}{d_6} + d_7 \cos \frac{2\pi(t - d_8)}{d_9}$$

This function is calibrated against global mean temperature data from 1880 provided in [Lenssen et al. \(2019\)](#). In the calibration, we have subtracted from the data the short-term variations of radiative forcing associated with the 11 year solar cycle and the transient reduction in global mean temperature following large volcanic eruptions, because we are more interested in the long-term trend of global mean temperature and thus including the short-term variation is not necessary in our opinion.

Table A4: Parameters values in the “No-New-Policy” global mean temperature fit

Symbol	Value	Units	Description
d_1	5.62	°C	Logistic function coefficient
d_2	2084	Julian year	Year of linear growth
d_3	42.6	Years	Growth timescale
d_4	0.16	°C	Long period amplitude
d_5	2058	Julian year	Year of long period maximum
d_6	161.5	Years	Long period
d_7	0.07	°C	Multidecadal oscillation amplitude
d_8	2058	Julian year	Year of maximum multidecadal oscillation
d_9	58.7	Years	Multidecadal oscillation period

C Economic Impacts of Climate Change

We divide climate change impacts into eight categories and calibrate them separately. We use $\langle CO_2 \rangle$ to represent the atmospheric carbon concentration which is proportional to the atmospheric carbon content c_a . Table A5 and Table A6 show the parameter values.

C.1 Agriculture

Impacts on agriculture production consist of three parts: adaption to changes in temperature, overall production associated with current temperature and soil fertilization by increase in atmospheric carbon dioxide concentration:

$$h_{i,t}^{AG} = h_{i,t}^{AG,\dot{\tau}} + h_{i,t}^{AG,\tau} + h_{i,t}^{AG,\langle CO_2 \rangle}.$$

The adaption impact is mainly the unexpected cost on agriculture production due to the change in global temperature. This cost is mainly caused by the limited farsightedness of farmers to correctly anticipate the change in climate in order to adjust the corresponding production techniques. This impact is constant if the change in global temperature is constant over time. Any new change in $\dot{\tau}$ causes the adjustment of adaption cost towards a different equilibrium level. The dynamic of this adaption cost is characterized by:

$$\dot{h}_{i,t}^{AG,\dot{\tau}} = \alpha_r \dot{\tau}^2 - \frac{h_{i,t}^{AG,\tau'}}{10},$$

with $\dot{h}_{i,1990}^{AG,\dot{\tau}} = 0$. Solving the above differential equation yields

$$h_{i,t}^{AG,\dot{\tau}} = c_{i,1} \frac{e^{-(t-1990)/10} \int_{1990}^t e^{(k-1990)/10} (\dot{\tau}_k/0.04)^2 dk}{e^{-(t-1990)/10} \int_{1990}^{2020} e^{(k-1990)/10} (\dot{\tau}_k/0.04)^2 dk}.$$

The second impact term is the change in overall agriculture production associated with the global mean temperature level. This impact is quadratic since each region has an optimal global temperature for its agriculture production:

$$h_{i,t}^{AG,\tau} = c_{r,2} \frac{\tau_t - \tau_{1990}}{\tau_{2020} - \tau_{1990}} + c_{r,3} \left(\frac{\tau_t - \tau_{1990}}{\tau_{2020} - \tau_{1990}} \right)^2.$$

The third impact term is the positive but saturating effect of soil fertilization caused by increase in atmospheric carbon dioxide concentration $\langle CO_2 \rangle$:

$$h_{i,t}^{AG,\langle CO_2 \rangle} = c_{r,4} \frac{\ln \langle CO_2 \rangle_t - \ln \langle CO_2 \rangle_{1990}}{\ln \langle CO_2 \rangle_{2020} - \ln \langle CO_2 \rangle_{1990}},$$

where $\langle CO_2 \rangle_{1990} = 351.28$ ppm and $\langle CO_2 \rangle_{2020} = 415.3$ ppm are from Ding (2018).

The share of agriculture production depends negatively on per capita income. To convert impact on agriculture production to total production, we have

$$\Omega_{i,t}^{AG} = h_{i,t}^{AG} \times \left(\frac{y_{i,t}}{y_{i,2020}} \right)^{-\zeta_r}.$$

The income elasticities of the share of agriculture production ζ_i are estimated using log-linear fit to FAOSTAT data²⁵ provided by the Food and Agriculture Organization of the United Nations.

C.2 Forestry

Impacts on forestry affects consumer and producer surplus that depend both on the global temperature increase and the atmospheric carbon dioxide concentration:

$$h_{i,t}^{FR} = c_{r,5} \frac{\tau_t - \tau_{1990}}{\tau_{2020} - \tau_{1990}} + c_{i,6} \frac{\ln \langle CO_2 \rangle_t - \ln \langle CO_2 \rangle_{1990}}{\ln \langle CO_2 \rangle_{2020} - \ln \langle CO_2 \rangle_{1990}}.$$

Unlike the agriculture, there is not enough evidence that the income elasticity of the share of forestry production is region-dependent, and hence

$$\Omega_{i,t}^{FR} = h_{i,t}^{FR} \times \left(\frac{y_{i,t}}{y_{i,2020}} \right)^{\epsilon_5}.$$

C.3 Water Resources

Climate change affects regional patterns of precipitation and evapotranspiration, and thus availability and cost of water supplies:

$$h_{i,t}^{WT} = c_{i,7} \left(\frac{y_{i,t} P_{i,t}}{y_{i,2020} P_{i,2020}} \right)^{1+\epsilon_7} e^{-\frac{1}{\nu_7}(t-2020)} \frac{\tau_t - \tau_{1990}}{\tau_{2020} - \tau_{1990}},$$

²⁵<http://www.fao.org/faostat>, accessed September 11, 2017.

where the exponential term represents the assumed technological progress on the efficiency of water delivery system. This part of estimation has high level of uncertainty mainly due to uncertain extrapolations of precipitation, evapotranspiration and hydrology at regional levels. We selected the parameter values to match [Anthoff and Tol \(2014\)](#) with exception being the parameters for CHI, FSU, WEU and CEE regions where we have noticed anomalies in [Anthoff and Tol \(2014\)](#)'s results and have adjusted parameter accordingly.

The impact $h_{i,t}^{WT}$ measures the dollar-value cost. To convert it to the percentage change in production, we have

$$\Omega_{i,t}^{WT} = h_{i,t}^{WT} / \left(\frac{y_{i,t} P_{r,t}}{y_{i,2020} P_{i,2020}} \right).$$

C.4 Heating, Cooling and Ventilation

Global warming reduces the energy required for heating, but such effect will eventually be saturated. On the other hand, it increases the energy consumption on cooling. In case when the global temperature declines to a lower-than-preindustrial level, i.e., $\tau = 0$, by implementation of SRM or any other climate intervention actions, we assume that the cooling cost stops growing:

$$\Omega_{i,t}^{HC} = \left(c_{i,8} \frac{\arctan(\tau_t - \tau_{1990})}{\arctan(\tau_{2020} - \tau_{1990})} + c_{i,9} \frac{\max\{\tau_t, 0\}^{1.5} - \tau_{1990}^{1.5}}{\tau_{2020}^{1.5} - \tau_{1990}^{1.5}} \right) \left(\frac{y_{i,t}}{y_{i,2020}} \right)^{\epsilon_8}.$$

The term $y_{i,t}^{-\epsilon}$ in the above formula includes two effects. The first effect accounts for the income elasticity of the share of energy consumption devoted to heating and cooling. The second effect accounts for the improvement of efficiency in these energy consumptions. Unlike the method in [Anthoff and Tol \(2014\)](#) that assumes this efficiency will improve indefinitely, we assume that it will eventually slow down and the pace of improvement is correlated with per capita income. The parameters in this formula are calibrated to match the results in [Anthoff and Tol \(2014\)](#) for global temperature increase at 1990-level, 2020-level and 2°C-level.

Increases in the atmospheric carbon dioxide concentration will also increase the ventilation requirements. We assume that the cost of limiting human exposure to elevated atmospheric carbon dioxide concentration grows linearly. Values for $c_{i,10}$ are based on [Bao et al. \(2018\)](#). The income elasticity of the share of this cost and its improvement on efficiency are assumed to be the same as the heating-cooling counterpart.

$$\Omega_{i,t}^{VT} = \left(c_{i,10} \frac{<CO_2>_t - <CO_2>_{1990}}{<CO_2>_{2020} - <CO_2>_{1990}} \right) \left(\frac{y_{i,t}}{y_{i,2020}} \right)^{\epsilon_8}.$$

C.5 Sea Level Rise and Dry Land Protection

Sea level rise causes the loss of dry land. We assume that the cost of protecting dry land in terms of monetary value is linear in the sea level rise S_t and population $P_{i,t}$:

$$h_{i,t}^{SL} = c_{i,11} \left(\frac{P_{i,t}}{P_{i,2020}} \right) \frac{S_t - S_{1990}}{S_{2020} - S_{1990}},$$

and the dynamic of sea level rise is based on [Grinsted et al. \(2010\)](#):

$$\dot{S}_t = \frac{1.2(\tau_t - \tau_{1990}) + 0.77 - S_t}{208},$$

with $S_{1990} = 0$ and $S_{2020} = 0.136$. To convert monetary value to percentage change in production, we have

$$\Omega_{i,t}^{SL} = h_{i,t}^{SL} / \left(\frac{y_{i,t} P_{i,t}}{y_{i,2020} P_{i,2020}} \right).$$

C.6 Ocean Acidification and Coral Reef Loss

Increase in atmospheric carbon dioxide concentration changes the surface layer acidity. The change in ocean layer pH from preindustrial value is approximated by

$$pH_t = 0.248 \cdot \left(\frac{<CO_2>_t}{280} - 1 \right)^{0.67}.$$

Based on [Brander et al. \(2012\)](#), the fractional loss of coral reef areas follows

$$R_t = \frac{0.56 \cdot pH_t}{1 + 0.56 \cdot pH_t}.$$

The monetary value on the fractional loss of coral reef area is estimated to be

$$h_{i,t}^{CR} = c_{i,12} \frac{R_t - R_{1990}}{R_{2020} - R_{1990}},$$

where values for $c_{i,12}$ are obtained by combining the estimations of coral reef areas and value per square kilometer in [Brander et al. \(2012\)](#). Converting it to the percentage change in production, we have

$$\Omega_{i,t}^{CR} = h_{i,t}^{CR} / \left(\frac{y_{i,t} P_{i,t}}{y_{i,2020} P_{i,2020}} \right).$$

C.7 Diseases

Climate change impacts on diseases are mainly associated with the increase in global temperature. We include impacts on mortality and morbidity caused by diarrhea, and on mortality caused by three vector-borne diseases: malaria, dengue fever and schistosomiasis:

$$\Omega_{i,t}^{DS} = \Omega_{i,t}^{diarrhea} + \Omega_{i,t}^{vector}.$$

We assume that economic impact of both mortality and morbidity associated with diarrhea increase linearly as the global temperature increases:

$$\Omega^{diarrhea} = \left[\underbrace{c_{i,13} \left(\frac{y_{i,t}}{y_{i,2020}} \right)^{\epsilon_{13}}}_{\text{mortality}} + \underbrace{c_{i,14} \left(\frac{y_{i,t}}{y_{r,2020}} \right)^{\epsilon_{14}}}_{\text{morbidity}} \right] \cdot \frac{\tau_t - \tau_{1990}}{\tau_{2020} - \tau_{1990}} e^{-\frac{1}{\nu_{13}}(t-2020)},$$

where the exponential term represents the global biomedical progress that reduces the impact from diarrhea and the value for ν_{13} is from [GBD 2016 Diarrhoeal Disease Collaborators \(2018\)](#).

The impact estimate for mortality associated with the vector-borne diseases is similar while the global biomedical progress parameter is obtained from Our World in Data²⁶:

$$\Omega^{vector} = c_{i,15} \left(\frac{y_{i,t}}{y_{i,2020}} \right)^{\epsilon_{15}} \cdot \frac{\tau_t - \tau_{1990}}{\tau_{2020} - \tau_{1990}} e^{-\frac{1}{\nu_{15}}(t-2020)}.$$

C.8 Storm

For simplicity, we assume that the economic impacts from tropical and extratropical storms are linear in global temperature increase:

$$\Omega_{i,t}^{ST} = c_{i,16} \left(\frac{y_{i,t}}{y_{i,2020}} \right)^{\epsilon_{16}} \cdot \frac{\tau_t - \tau_{1990}}{\tau_{2020} - \tau_{1990}}.$$

Table A5: Parameter values for ϵ_n , ν_n and ζ_i in climate change impact assessment

n:	1	2	3	4	5	6	7	8	9	10	11	12	13	14	15	16
ϵ_n	-	-	-	-	0.31	-	-0.15	-1.00	-	-	-	-	-1.58	-0.42	-2.65	-0.51
ν_n	-	-	-	-	-	-	138.60	-	-	-	-	-	30.00	-	16.00	-
Region:	USA	CAN	WEU	JPK	ANZ	CEE	FSU	MDE	CAM	SAM	SAS	SEA	CHI	NAF	SSA	SIS
ζ_i	0.80	3.00	1.96	1.01	4.01	2.07	1.47	1.59	0.43	2.23	0.96	1.42	1.19	1.57	1.31	3.12

²⁶<https://ourworldindata.org/malaria>, accessed August 4, 2019.

Table A6: Parameter values for $c_{i,k}$ in climate change impact assessment

k:	USA	CAN	WEU	JPK	ANZ	CEE	FSU	MDE
1	-.00079	-.00249	-.00147	-.00026	-.00111	-.00175	-.00212	-.00095
2	.01882	.12107	.01704	.00783	.07069	.06152	.08877	.03643
3	-.00647	-.01981	-.00761	-.00269	-.01707	-.01684	-.02714	-.01062
4	.01320	.00902	.02596	.00914	.04682	.02562	.02696	.01733
5	.00192	.00039	.00088	.00150	-.00444	.00194	-.00075	0
6	.00019	.00004	.00009	.00015	-.00048	.00021	-.00008	0
7	-.03290	-.02884	-.03414	.00016	.00015	-.03440	-.03106	-.06408
8	.27674	.24680	.15804	.13493	.09660	.29902	1.14978	.13456
9	-.12088	-.10734	-.21562	-.01671	-.01187	-.10723	-.41189	-.13388
10	-.14389	-.12778	-.12765	-.01989	-.01414	-.12765	-.49032	-.15937
11	-.00012	-.00018	-.00021	-.00028	-.00063	-.00003	-.00027	-.00006
12	-.00001	0	0	-.00011	-.00658	0	0	-.00037
13	-.01427	-.01570	-.00594	-.00340	-.00033	-.00713	-.07341	-.01109
14	-.00254	-.00261	-.00098	-.00025	-.00012	-.00131	-.01162	-.00025
15	-.00001	-.00001	-.00005	-.00060	-.00002	-.00007	-.00004	-.00593
16	-.00916	-.00017	-.00015	-.00265	-.00160	-.00004	-.00018	-.00002
k:	CAM	SAM	SAS	SEA	CHI	NAF	SSA	SIS
1	-.00176	-.00080	-.00029	-.00009	-.00028	-.00149	-.00125	-.00117
2	.08670	.00727	.01337	.00444	.01806	.06216	.07176	.03081
3	-.02240	-.00514	-.00333	-.00140	-.00528	-.01880	-.01638	-.00571
4	.06197	.04154	.00836	.00923	.01667	.02931	.04207	.05542
5	.00061	.00084	.00297	.00304	.00585	0	.00036	0
6	.00007	.00009	.00035	.00032	.00059	0	.00004	0
7	-.06595	-.07115	-.06707	-.14010	0	-.43965	-.17835	-.06687
8	.24589	.26098	.19457	.38741	1.81056	.00973	.00416	.24143
9	-.14193	-.18005	-.21778	-.43402	-1.38006	-1.29171	-.58148	-.16589
10	-.06378	-.06534	-.14026	-.07142	-.05267	-.08266	-.42247	-.08140
11	-.00037	-.00045	-.00033	-.00044	-.00011	-.00019	-.00078	-.00064
12	-.00041	-.00010	-.00034	-.00497	-.00004	-.00035	-.00119	-.02098
13	-.07772	-.07062	-.01927	-.01482	-.00069	-.15122	-1.94971	-.1046
14	-.00104	-.00010	-.00092	-.00069	-.00029	-.00150	-.00991	-.00171
15	-.00152	-.00129	-.00110	-.00074	-.00005	-.07587	-.46381	-.02272
16	-.01157	-.00013	-.01064	-.00363	-.00485	-.00001	-.00106	-.04317

D Proof of Theorem 1

To simplify notations, we will drop the region index from the variables. We can write the change in the region's social welfare from the background economy as

$$\begin{aligned}
& \int_{t_0}^{\infty} P \frac{(C^*/P)^{1-\theta}}{1-\theta} e^{-\rho(t-t_0)} dt - \int_{t_0}^{\infty} P \frac{(C^0/P)^{1-\theta}}{1-\theta} e^{-\rho(t-t_0)} dt \\
&= \int_{t_0}^{\infty} P^\theta \left(\frac{(C^*)^{1-\theta} - (C^0)^{1-\theta}}{1-\theta} \right) e^{-\rho(t-t_0)} dt \\
&\approx \int_{t_0}^{\infty} P^\theta \left(\frac{(C^0)^{1-\theta} + (1-\theta)(C^0)^{-\theta}(C^* - C^0) - (C^0)^{1-\theta}}{1-\theta} \right) e^{-\rho(t-t_0)} dt \\
&= \int_{t_0}^{\infty} P^\theta (C^0)^{-\theta} (C^* - C^0) e^{-\rho(t-t_0)} dt \\
&= \epsilon \int_{t_0}^{\infty} P^\theta (C^0)^{1-\theta} \cdot \gamma \cdot e^{-\rho(t-t_0)} dt,
\end{aligned}$$

where the approximation holds when $\epsilon\gamma$ is small.

To characterize the relative perturbation terms, let us define the *control theory Hamiltanian*:

$$\mathcal{H}(C, K, \lambda) := \lambda(t) \cdot (Y(t) - rK(t) - C(t)) + L_t \frac{(C(t)/L_t)^{1-\theta}}{1-\theta} e^{-\rho(t-t_0)},$$

where λ is the *costate variable*. Suppose C^* is the solution to the optimization problem and K^* is the corresponding state variable, the *Pontryagin's Maximum Principle* implies that there exists λ^* such that²⁷

$$\begin{cases} \dot{K}^*(t) &= \mathcal{H}_\lambda(C^*, K^*, \lambda^*); \\ \dot{\lambda}^*(t) &= -\mathcal{H}_K(C^*, K^*, \lambda^*); \\ C^*(t) &= \arg \max_{C(t)} \mathcal{H}(C, K^*, \lambda^*); \\ \lim_{t \rightarrow \infty} \lambda^*(t) &= 0, \end{cases}$$

where \mathcal{H}_λ and \mathcal{H}_K are the partial derivative of \mathcal{H} with respect to λ and K , respectively. The first condition is simply the constraint of the optimization problem. The second condition implies

$$\dot{\lambda}^*(t) = - \left(\frac{(1-\omega)Y^*(t)}{K^*(t)} - r \right) \cdot \lambda^*(t),$$

and the third condition implies

$$\begin{cases} \lambda^*(t) = L_t^\theta C^*(t)^{-\theta} e^{-\rho(t-t_0)} &, \text{ if } \lambda^*(t) > 0; \\ C^*(t) = Y^*(t) + (1-r)K^*(t) &, \text{ if } \lambda^*(t) \leq 0. \end{cases}$$

²⁷The Pontryagin's Maximum Principle is only proved for finite-horizon optimal control problems. Here we assume that the solution to the original infinite-horizon optimization problem can be approximated as $T \rightarrow \infty$. Tauchnitz (2015) points out that such direct application of the Pontryagin's Maximum Principle to infinite-horizon optimal control problems may cause some issues in certain situations. We have no intention to formally tackle these issues since our primary concern will be to characterize the perturbation of the solution caused by climate impact D . This caveat is nonetheless pointed out here for future work.

Assuming the costate variable λ^* never declines to zero, we will thus have the following *Euler-Lagrange equation*:

$$\frac{(1-\omega)Y^*(t)}{K^*(t)} - \frac{\theta\dot{C}^*(t)}{C^*(t)} = r + \rho - \frac{\theta\dot{L}_t}{L_t}.$$

In addition, since the Euler-Lagrange equation must also be satisfied by the background economy in which $D_t \equiv 0$, we therefore must have

$$\frac{(1-\omega)Y^*(t)}{K^*(t)} - \frac{\theta\dot{C}^*(t)}{C^*(t)} = \frac{(1-\omega)Y_t^0}{K_t^0} - \frac{\theta\dot{C}_t^0}{C_t^0}. \quad (18)$$

Notice that we have

$$\begin{aligned} \frac{Y^*(t)}{K^*(t)} &= (1 + \epsilon D_t) A_t (K^*(t))^{-\omega} L_t^\omega \\ &= \frac{Y_t^0}{K_t^0} \cdot (1 + \epsilon D_t) \cdot (1 + \epsilon \kappa(t))^{-\omega} \\ &= \frac{Y_t^0}{K_t^0} \cdot (1 + \epsilon D_t)(1 - \omega \epsilon \kappa(t) + O(\epsilon^2)) \\ &= \frac{Y_t^0}{K_t^0} \cdot (1 + \epsilon D_t - \omega \epsilon \kappa(t) + O(\epsilon^2)), \end{aligned}$$

where $O(\epsilon^2)$ means that the error term is of second order for ϵ . In addition, we also have

$$\begin{aligned} \frac{\dot{C}^*(t)}{C^*(t)} &= \frac{\epsilon \dot{\gamma}(t) C_t^0 + (1 + \epsilon \gamma(t)) \dot{C}_t^0}{(1 + \epsilon \gamma(t)) C_t^0} \\ &= \frac{\dot{C}_t^0}{C_t^0} + \frac{\epsilon \dot{\gamma}(t)}{1 + \epsilon \gamma(t)}. \end{aligned}$$

Combining these two derivations, equation (18) becomes

$$\frac{(1-\omega)Y_t^0}{K_t^0} \cdot (\epsilon D_t - \omega \epsilon \kappa(t) + O(\epsilon^2)) = \theta \cdot \frac{\epsilon \dot{\gamma}(t)}{1 + \epsilon \gamma(t)}.$$

Multiplying both sides by $(1 + \epsilon \gamma)/\epsilon$ yields

$$\begin{aligned} \theta \dot{\gamma} &= \frac{(1-\omega)Y_t^0}{K_t^0} \cdot (1 + \epsilon \gamma(t)) \cdot (D_t - \omega \kappa(t) + O(\epsilon)) \\ &= \frac{(1-\omega)Y_t^0}{K_t^0} \cdot (D_t - \omega \kappa(t) + O(\epsilon)) \end{aligned} \quad (19)$$

Using similar idea, the constraint in the maximization problem can be written as

$$(1 + \epsilon \kappa) \dot{K}^0 + \epsilon \dot{\kappa} K^0 = (1 + \epsilon D)(1 + \epsilon \kappa)^{1-\omega} Y^0 - (1 + \epsilon \kappa) r K^0 - (1 + \epsilon \gamma) C^0.$$

Since this constraint also holds for the background economy, we must also have $\dot{K}^0 = Y^0 - r K^0 - C^0$.

Combining this observation with the above equation, we then have

$$\begin{aligned}\epsilon\kappa\dot{K}^0 + \epsilon\dot{\kappa}K^0 &= [(1+\epsilon D)(1+\epsilon\kappa)^{1-\omega} - 1] Y^0 - \epsilon\kappa r K^0 - \epsilon\gamma C^0 \\ &= [(1+\epsilon D)(1+(1-\omega)\epsilon\kappa + O(\epsilon^2)) - 1] Y^0 - \epsilon\kappa r K^0 - \epsilon\gamma C^0 \\ &= (\epsilon(1-\omega)\kappa + \epsilon D + O(\epsilon^2))Y^0 - \epsilon\kappa r K^0 - \epsilon\gamma C^0.\end{aligned}$$

Dividing both sides by ϵ , we have

$$\begin{aligned}K^0\dot{\kappa} &= ((1-\omega)\kappa + D + O(\epsilon))Y^0 - (rK^0 + \dot{K}^0)\kappa - C^0\gamma \\ &= ((1-\omega)\kappa + D + O(\epsilon))Y^0 - (Y^0 - C^0)\kappa - C^0\gamma \\ &= (D - \omega\kappa + O(\epsilon))Y^0 - (\gamma - \kappa)C^0\end{aligned}$$

Dividing both sides by K^0 and collecting coefficients for κ and γ , we then have

$$\dot{\kappa} = \left[-\omega \frac{Y^0}{K^0} + \frac{C^0}{K^0} \right] \kappa - \frac{C^0}{K^0} \gamma + (D + O(\epsilon)) \frac{Y^0}{K^0} \quad (20)$$

Omitting the small error term $O(\epsilon)$ in equation (19) and (20) yields the equation (14).

Since the total productivity and labor input are proportional to a logistic function that will approach a constant in the limit, we can see from Lemma 1 that the background economy will approach a steady state in the limit. When we have $\lim_{t \rightarrow \infty} D(t) = \bar{D}$, then we can rewrite equation (14) in the limit as

$$\begin{cases} \dot{\gamma}(t) &= \Gamma_1 + \Gamma_2\kappa(t); \\ \dot{\kappa}(t) &= \Gamma_3 + \Gamma_4\kappa(t) - \Gamma_5\gamma(t). \end{cases}$$

This pair of linear differential equations has a stable steady state:

$$\begin{cases} \bar{\gamma}(t) &= -\frac{\Gamma_1}{\Gamma_2} \\ \bar{\kappa}(t) &= \frac{\Gamma_3}{\Gamma_5} - \frac{\Gamma_1\Gamma_4}{\Gamma_2\Gamma_5}. \end{cases}$$

Therefore, we must have

$$\lim_{t \rightarrow \infty} \dot{\kappa}_r(t) = 0.$$